STUART LITTLE NO MORE: EFFECTS OF HIGH RESISTANCE WHEEL RUNNING ON SKELETAL MUSCLE HYPERTROPHY AND STRENGTH IN C57BL/6 MICE

A Thesis
By
PIETER JAN KOOPMANS

Submitted to the School of Graduate Studies
at Appalachian State University
in partial fulfillment of the requirements for the degree of
MASTER OF SCIENCE

May 2022
Department of Health and Exercise Science

STUART LITTLE NO MORE: EFFECTS OF HIGH RESISTANCE WHEEL RUNNING ON SKELETAL MUSCLE HYPERTROPHY AND STRENGTH IN C57BL/6 MICE

A Thesis
by
PIETER JAN KOOPMANS
May 2022

APPROVED BY:

Kevin Zwetsloot, Ph.D.
Chairperson, Thesis Committee

R. Andrew Shanely, Ph.D.
Member, Thesis Committee

N. Travis Triplett, Ph.D.
Member, Thesis Committee

Kelly Cole, Ph.D.
Chairperson, Department of Exercise Science

Marie Hoepfl, Ed.D.
Interim Dean, Cratis D. Williams School of Graduate Studies

Abstract

STUART LITTLE NO MORE: EFFECTS OF HIGH RESISTANCE WHEEL RUNNING ON SKELETAL MUSCLE HYPERTROPHY AND STRENGTH IN C57BL/6 MICE

Pieter Jan Koopmans
B.S., University of Wisconsin- La Crosse
M.S., Appalachian State University

Chairperson: Kevin Zwetsloot, Ph.D.

Skeletal muscle mass comprises approximately 40% of body mass in adult humans; thus, maintaining skeletal muscle mass throughout the lifespan is critical to maintain normal function and health. To study the molecular and cellular mechanisms of maintaining muscle mass, animal models have been utilized as the physiological adaptations to resistance exercise are ubiquitous across mammalian species. Animal models have the benefit of strong control over diet and exercise regimen. Further, the collection of whole tissues from animal models, such as brain, liver, heart, and skeletal muscle, allow for greater depth of exploration into the molecular and cellular mechanisms that regulate muscle mass. As such, many resistance-based exercise models have been developed for use in rodents: synergistic ablation (Goldberg, 1968) electrical stimulation (Baar & Esser, 1999), weighted ladder climbing (Hornberger Jr. & Farrar, 2004), and canvassed squatting (Tamaki et al., 1992).
While these models are valuable, they are also invasive, tedious, involuntary, and manpower intensive. Fortunately, many rodent strains voluntarily run long distances when given access to a running wheel. To mimic human resistance exercise models, external resistance can be applied to the running wheel and progressively increased. Numerous studies have demonstrated that loaded wheel running models can induce adaptations commonly seen with

resistance exercise in humans, such as increased enzymatic activity, muscle hypertrophy, and stimulation of muscle protein synthesis (D'Hulst et al., 2019; Dungan et al., 2019; Legerlotz et al., 2008; C. B. Mobley et al., 2018).

The literature examining hypertrophic adaptations with mice at low to moderate resistances is abundant (Allen et al., 2001; Ishihara et al., 2002; Lerman et al., 2002; Soffe et al., 2016); however, responses to high wheel resistances (>50% of body mass) are scant. Further, loaded wheel running models in mice involving the addition of low to moderate wheel load often fail to deter mice from running great distances, which is more reflective of an endurance/resistance training model (Murach et al., 2020). Elucidation of hypertrophic responses to high resistances, which may further bias the training stimulus towards resistance training may help improve the effectiveness of the loaded wheel running model in mice, and consequently, future research in this field.

Thus, the purposes of this study were to: 1) characterize the running patterns of C57BL/6 mice utilizing the voluntary progressive loaded wheel running model at higher than previously used loads, 2) assess muscle hypertrophy and strength in response to free wheel running (FWR), loaded wheel running (LWR), and high loaded wheel running (HLWR).

Acknowledgments

In no order of importance, I issue thanks to:

Dr. R. Andrew Shanely, Dr. Kevin Zwetsloot, and Dr. Travis Triplett for the guidance and support of my decision to take a year off in the middle of grad school due to circumstances surrounding the pandemic. I could go on about how wonderful my advisors have been but simply, I very much lucked into having compatible and caring advisors as a graduate student despite not knowing much about them or their research prior to working with them. As a pupil of theirs, I have always felt that their priority as mentors was to provide meaningful experiences and skills that translate well to future endeavors.

Next, my parents for dealing with me and letting me mooch off them for an additional year while I lived at home free of rent and grocery bills.

Monique Eckerd, Therin Williams-Frey, and Levi Hill for overseeing daily operations of the animal facility, observation/care of research animals, and assisting with cryotomy of muscle tissues.

The Office of Student Research, Graduate Student Government Association, and the Department of Health and Exercise Science for providing funding that allowed us to purchase materials for the running wheel apparati and IHC materials.

Table of Contents

Chapter 1. Introduction

Skeletal muscle mass comprises approximately 40% of body mass in adult humans; thus, maintaining skeletal muscle mass throughout life is critical. Skeletal muscle mass plays an integral role in energy metabolism, maintaining core body temperature, and glucose homeostasis (Frontera & Ochala, 2015). In older adults, low muscle mass is an indicator of functional impairment and disability (Janssen et al., 2002). Additionally, accelerated loss of muscle mass is predictive of all-cause mortality, regardless of age, lifestyle, and health status (Szulc et al., 2010). Maintenance of skeletal muscle is a balance between protein synthesis and protein degradation, but many gaps exist in our understanding of the intricate molecular and cellular mechanisms that drive this process. Therefore, biomedical research elucidating these underlying mechanisms is of great importance.

To study the molecular and cellular mechanisms of maintaining muscle mass, research involving human subjects often employs resistance exercise-based interventions as mechanical stimuli play an integral role in the regulation of skeletal muscle mass. While human subjects research in this area has been successful, the time necessary to exhibit adaptations and ethical concerns limit the quantity of data that can be obtained. The physiological adaptations to resistance exercise are fairly ubiquitous across species and animal models have the benefit of being able to precisely control the diet and exercise regimen. Furthermore, the collection of whole tissues from animal models, such as brain, liver, heart, and skeletal muscle, allow for greater depth of exploration into the molecular and cellular mechanisms that regulate muscle mass.

Many resistance-based exercise models have been developed for use in rodents:

- Synergistic ablation (Goldberg, 1968) - the surgical alteration of the gastrocnemius requiring compensatory hypertrophy from synergist muscles
- Electrical stimulation (Baar & Esser, 1999; Wong & Booth, 1988) - insertion of an electrode into the sciatic nerve and direct stimulation of the lower leg to contract against a weighted pulley
- Weighted ladder climbing (Duncan et al., 1998; Hornberger Jr. & Farrar, 2004; Lee et al., 1987; Yarasheski et al., 1990) - rats are operantly conditioned to climb up a steep ladder with known masses attached to their tail.
- Weighted Pulling (Zhu et al, 2021) - mice are trained to pull a weighted cart along a short track
- Canvassed squatting (Tamaki et al., 1992) - rats wear a weighted canvas jacket over their torso and electrical stimulus is provided to make the animal extend its legs, performing a squat-like movement.

While these models are valuable, they are also invasive, tedious, involuntary, and require a sufficient amount of manpower. Fortunately, many rodent strains voluntarily run long distances when given access to a running wheel and do not rely on positive/negative reinforcement or anesthesia to force movement (De Bono et al., 2006; Goh & Ladiges, 2015; Lightfoot et al., 2004; Meijer & Robbers, 2014). The design of the running wheel is similar to a hamster exercise wheel, which is a solid or mesh wheel that rotates about an axle. To mimic human resistance exercise models, external resistance/load can be applied to the running wheel and the resistance/load can be progressively increased. Numerous studies have found that free wheel running (FWR) and loaded wheel running (LWR) models are capable

of inducing adaptations commonly seen with resistance exercise in humans, such as increased enzymatic activity, muscle hypertrophy, strength increases, and stimulation of muscle protein synthesis (MPS; Allen et al., 2001; Call et al., 2017; D'Hulst et al., 2019; Ishihara et al., 1998, 2002; Legerlotz et al., 2008; C. B. Mobley et al., 2018; Sexton, 1995; White et al., 2016). As animal handling and stress is minimal and muscular adaptations are similar to previously studied involuntary models, FWR and LWR are considered a viable model of resistance exercise training in rodents (Manzanares et al., 2018).

The hypertrophic responses to the FWR and LWR models reported in the relatively limited number of studies thus far are inconsistent, especially in mice, perhaps due to variations in progressive overload employed in LWR models. Additionally, LWR rat models tend to use higher resistance than LWR mouse models; 40-173% of body mass versus 5-41% of body mass (Konhilas et al., 2005; Legerlotz et al., 2008). Literature examining hypertrophic adaptations with mice at low to moderate resistances is abundant (Allen et al., 2001; Call et al., 2017; D'Hulst et al., 2019; Ishihara et al., 2002; Lerman et al., 2002; Soffe et al., 2016); however, responses to high wheel resistances (>50% of body mass) are scant. Elucidation of hypertrophic responses to high resistances may help improve the effectiveness of the LWR model in mice, and consequently, future research in this field.

Purpose of Study

The purposes of this study are to: 1) to characterize the running patterns- distance, duration, and velocity of male C57BL/6 mice utilizing voluntary progressive loaded wheel running model at higher than previously used loads and 2) assess muscle hypertrophy and strength in response to free wheel running (FWR), loaded wheel running (LWR), and high loaded wheel running (HLWR).

Hypotheses

I hypothesize that: 1a) the LWR treatment would not cause a decrease in running distance compared to FWR , 1b) HLWR treatment would cause a decrease in running distance compared to FWR and LWR, 2a) FWR treatment will display greater strength than SED group, 2b) LWR and HLWR treatment will display greater muscular strength than FWR and SED treatment, 3a) FWR group will display greater muscle mass and fCSA than SED group, 3b) LWR and HLWR groups will display greater muscle mass and fCSA than FWR and SED treatments

Chapter 2 Literature Review

Function of Muscle Mass

Skeletal muscle is tissue that comprises approximately 40% of body mass in adult humans and plays an integral role in mechanical and metabolic functions (Frontera & Ochala, 2015); thus, maintenance of it throughout life is critical. Skeletal muscle contains muscle fibers that consist of sarcomeres which are the smallest repeating functional unit of the muscle. Myosin proteins possess ATPase enzymes that produce force by forming cross-bridges with actin, pulling the Z-disks towards the M-line, resulting in the shortening of the sarcomere (Huxley, 1969). The combined shortening of sarcomeres at the whole-muscle scale generates the muscular contraction and relaxation action, which enables the body to perform a large swath of movements.

Loss of muscle mass can contribute to osteoporosis. Mechanical forces on the bone are essential for regulating remodeling processes; and the greatest forces come from muscular contraction (Frost, 1997). The Mediterranean Intensive Oxidant Study reports that skeletal muscle mass is positively correlated with bone mineral content/density and that men with the least muscle mass had increased risk of falls due impaired balance, presumably because of decreased muscle strength (Szulc et al., 2004). Sarcopenia is a loss of muscle mass and function that progresses with aging and can reduce mobility and quality of life. The decline is muscle mass and function represent one of the most prominent changes during the aging process. The cause of sarcopenia has not yet been fully elucidated but some of the proposed mechanisms are decreased satellite cell proliferation, physical inactivity, hormonal status (decreased production of androgenic sex hormones), and blunted protein synthesis in response to exercise and feeding (Cuthbertson et al., 2006; Larsson et al., 2019).

Skeletal muscle stores large amounts of glycogen, amino acids, and triglycerides and is involved in a host of metabolic pathways, such as glycolysis, citric acid cycle, beta oxidation, and mitochondrial respiration. As previously mentioned, skeletal muscle plays a central role in protein metabolism by serving as a reservoir for amino acids, allowing protein synthesis to be maintained in the absence of amino acids that are received from food (Wolfe, 2006). Furthermore, muscles exert autocrine, paracrine, and endocrine functions by excreting myokines, which allows them to support the metabolic functioning of different tissues, including adipose tissue, bones, liver, and pancreas (Schnyder & Handschin, 2015). Skeletal muscle mass also plays a role in chronic disease, such as heart failure, cancer cachexia, Type II diabetes, osteoporosis, and sarcopenia. Heart failure and cancer cachexia are associated with rapid loss of muscle mass, with the loss of muscle mass being a determinant of survival. In lung cancer patients receiving radiation treatment, patients who had a loss in body protein had an earlier recurrence of disease and lower rate of survival than those whose body protein increased (Kadar et al., 2006). Skeletal muscle is the primary site for insulin-stimulated glucose uptake from the blood making it essential in maintaining glucose homeostasis (DeFronzo & Tripathy, 2009). Lower muscle mass can reduce the capacity to uptake glucose from the blood, is associated with poor insulin sensitivity, and higher risk of developing Type II diabetes (S. Hong et al., 2017), a disease characterized by a decreased ability of insulin to stimulate the uptake of glucose from blood (Reaven, 2005).

Skeletal Muscle Plasticity

Skeletal muscle is an incredibly plastic tissue and adapts in response to many stimuli. It is well known that exercise plays a key role in the maintenance of muscle mass and can provide distinct adaptations that are dependent on the modality of exercise.

Adaptations to Endurance Exercise Training

During endurance exercise, energy is supplied mostly through aerobic respiration and thus adaptations reflect the need for increased oxygen supply and Adenosine Triphosphate (ATP) production. Some of the hallmark adaptations are increases in mitochondrial content, enzymatic activity, capillary density, and fiber type transitions (J O Holloszy & Booth, 1976).

The first study to demonstrate that endurance exercise induces adaptations to mitochondria was performed on rats that were trained to slowly adapt to a 2hr/day running program (Holloszy, 1967). They demonstrated that the capacity of mitochondria in the gastrocnemius muscle to oxidize pyruvate doubled, with total protein content of mitochondria increasing by 60%. Enzyme activity per gram of tissue also doubled in hindlimb muscles in response to training: succinate dehydrogenase, nicotinamide adenine dinucleotide (NADH) dehydrogenase, NADH-cytochrome c reductase, and cytochrome oxidase (Holloszy, 1967). The increased mitochondrial content and enzyme activity allows for a greater respiratory capacity, potentially yielding greater production of ATP per unit time.

A major regulator of mitochondrial adaptations is peroxisome proliferator-activated gamma coactivator-1-alpha (PGC-1α; Lira et al., 2010). PGC-1α is a transcriptional factor that targets genes responsible for mitochondrial biogenesis. Its expression is regulated by several upstream kinases that are activated during endurance exercise such as Calcium/ Calmodulin-dependent protein kinase (CamK), adenosine monophosphate-activated protein kinase (AMPK), and P38 mitogen-activated protein kinase (P38MAPK) which are activated by increases in intracellular calcium, reactive oxygen species (superoxide, hydrogen

peroxide), and ATP turnover, respectively. PGC-1α is controlled under a feed-forward regulatory loop that leads to enhanced expression of itself via its interaction with myocyte enhancer factor 2 on its own promoter (Handschin et al., 2003).

Increased levels of enzymes required for fatty acid oxidation and the citric acid cycle have also been observed as an adaptation to endurance exercise (Chi et al., 1983; P. Schantz et al., 1983). An additional result of these mitochondrial and enzymatic adaptations is that an absolute exercise intensity requires a smaller percentage of the muscles' maximal respiratory capacity. Furthermore, a right-hand shift in substrate utilization exists in response to endurance exercise training with increased utilization of lipids and a decreased utilization of carbohydrates at submaximal exercise intensities (Kiens et al., 1993). Additionally, following high-intensity interval training, skeletal muscle hydrogen ion buffering capacity has been shown to increase (Weston et al., 1996).

Skeletal muscle capillary density has also been shown to increase in response to endurance exercise (Brodal et al., 1977; Sexton, 1995). A consequence of skeletal muscle capillarization is improved oxygen and substrate delivery to muscle tissue. Exercise-induced skeletal muscle capillarization is regulated by several pathways, the most essential of which is vascular endothelial growth factor pathway (VEGF; Gavin, 2009). VEGF is a glycoprotein mitogen that predominantly binds to VEGF receptors on endothelial cells. Exercise increases the release of VEGF from muscle cells which eventually binds to two tyrosine kinase receptors. Several intracellular signals have been proposed to regulate VEGF expression and they occur predominantly through alterations to mRNA. One well known regulator or VEGF is hypoxia. When skeletal muscle cells are exposed to hypoxic conditions, expression of VEGF is increased; however, the response to hypoxia plateaus at around 55-65% of

maximum exercise intensity (Gavin, 2009). Another well-known regulator is nitric oxide, generated by nitric oxide synthase (NOS). Nitric oxide is released by endothelial cells during exercise and contributes to the blood flow response to exercise. When NOS is inhibited, the VEGF and VEGF receptors mRNA expression is decreased in response to acute endurance exercise (Gavin et al., 2000).

Changes in muscle fiber contractile properties exist as well, with numerous studies demonstrating that endurance exercise induces changes from a glycolytic to a more oxidative phenotype (Myosin heavy chain ATPase isoform IIx to IIa) in fast-twitch fibers. Although Myosin heavy chain type I and IIa isoforms coexist in human skeletal muscle fibers following endurance training, transitions to type I fibers have not been confirmed in research (Schantz & Dhoot, 1987; Yan et al., 2011). Although the slower isoforms lead to decreased force-producing capabilities, they also lead to improved metabolic efficiency, ultimately improving performance in endurance exercise.

Adaptations to Resistance Exercise Training

Resistance training is often used to improve sports performance and is known to elicit a broad spectrum of adaptations in various physiological systems. Adaptations include increases in muscle size and strength, muscle fiber type transitions, neuroendocrine function, and connective tissue (A. R. Hong & Kim, 2018; Kraemer et al., 1988; McGuigan et al., 2012; Young, 2006). The adaptations most pertinent to the scope of this study are increases in muscle size and strength. Muscular strength increases by several mechanisms both morphological and neurological. Neurological adaptations contribute to most of the early increases in muscular strength and include enhanced motor unit recruitment and firing rate, both of which are likely due to increased neural drive at the spinal or supraspinal level

(Folland & Williams, 2007). Adaptations to connective tissue include increased tendon stiffness and potentially increased plasticity of the connective tissue matrix surrounding skeletal muscle, having implications on enhanced rate of force development during the stretch-shortening cycle (Folland & Williams, 2007).

A primary morphological adaptation exhibited in response to resistance training is hypertrophy of the muscle fiber. The potential for muscle hypertrophy varies greatly on an individual basis (Bamman et al., 2007; Mobley et al., 2018b) potentially due to a large number of intrinsic and extrinsic factors such as diet, sleep, age, and genetics. Though in general, fiber cross sectional area (fCSA) has been shown to increase by 10-30% in response to 6-16 weeks of progressive resistance training (Bellamy et al., 2014; Hikida et al., 2000; Rosenberger et al., 2017). Macdougal et al. examined the myofibrillar structure of subjects before and after six months of strength training and found that myofilament concentration was unchanged (MacDougall et al., 1980). However recently, Haun et al. report despite fCSA increasing 23% in response to six weeks of high-volume resistance training, the actin and myosin concentration had decreased by 30% (Haun et al., 2019). Proteomic analyses indicated that there was expansion of sarcoplasmic proteins involved in glycolysis and other metabolic processes necessary for ATP production. These changes persisted after eight days of no training indicating that they are likely not due to edema. The discrepancy between the findings of these studies could be due to the time course of training, indicating that there may be a time-dependent expression of proteins whereby proteins necessary for energy production and transport precede myofibrillar elements.

Another morphological adaptation is the remodeling of sarcomeric structure to increase pennation angle (Aagaard et al., 2001). Change in pennation angle increases the

physiological CSA which represents the maximum number of cross-bridges that can be activated during muscular contraction, proportional to maximal force-producing capacity. Skeletal muscle fibers in humans exhibit three different myosin heavy chain (MHC) isoforms: type I, IIa, and IIx. They are commonly distinguished by myosin ATPase activity and staining with anti-MHC antibodies (Bloemberg & Quadrilatero, 2012). Several studies have found subtle muscle fiber type transitions, showing a decrease in the proportion of MHC IIx and increase in MHC IIa after 12-14 weeks of training (Andersen & Aagaard, 2000; Hakkinen et al., 1998; Williamson et al., 2001). This could be due to alterations in the predominant MHC in hybrid IIa/IIx fibers. Subsequent to detraining, these fiber type transitions are reversed and even "overshot" (Andersen & Aagaard, 2000). MHC II isoforms have greater force production potentially due to an increased number and stiffness of cross-bridges (Miller et al., 2015). Though MHC IIx fibers produce slightly more force than MHC IIa fibers, the motor units containing MHC IIa fibers have a lower recruitment threshold (Choi, 2014).

Concurrent Training

Several sports require the need for the development of multiple physical characteristics such as strength, power, and endurance; thus, the inclusion of both endurance and resistance exercise in a single training regimen is called concurrent training. Compared to resistance training alone, concurrent training has been shown to result in decrements in strength, hypertrophy, and power (Wilson et al., 2012). On the contrary, an opinion piece published by Dr. Murach and Bagley posited that there is zero experimental evidence for aerobic exercise training interfering with hypertrophic potential of resistance exercise training at the cellular or whole muscle level (Murach and Bagley, 2016). The extent of the

interference phenomenon is determined by training history, proximity of training sessions, and intensity and volume of endurance exercise training. The adaptations to resistance exercise and endurance exercise are very different so it is logical that the adaptations may interfere with one another. The molecular basis for this interference phenomenon is that protein synthesis pathways upregulated by resistance exercise are inhibited by protein degradation pathways that are upregulated by endurance training (Hawley, 2009). Additionally, residual fatigue from the previous exercise session may attenuate the capacity to maximally upregulate molecular pathways. The interference effect can be attenuated by separating training sessions, order of which does not seem to be of particular importance given total work performed by each modality is equal (Jones et al., 2016), though this recommendation may not be representative of the "real world" implications of training athletes.

Regulation of Skeletal Muscle Mass

Skeletal muscle mass is regulated by independent and interactive cellular signaling cascades. A balance between muscle protein synthesis (MPS) and muscle protein breakdown (MPB) needs to be maintained. Here, both sides of this balance are discussed below.

Muscle Protein Synthesis

The primary pathway for initiation of MPS is through Protein Kinase B (PKB, also known as AKT), a central hub of many anabolic and catabolic pathways, with the insulin receptor signaling pathway playing a significant role in many actions. The pathway begins with binding of insulin and insulin-like growth factors (IGFs) to the insulin receptor. This causes dimerization and subsequent autophosphorylation of the receptor followed by phosphorylation of several substrate proteins with insulin receptor substrate (IRS) being the

most important one. IRS proteins gather to enable phosphoinositol-3-kinase (PI-3k) to convert phosphatidylinositol-2-phosphate (PIP2) to PIP3. The increase in PIP3 signals for AKT to translocate to the plasma membrane for activation (Cork et al., 2018).

Furthermore, mechanical stimuli during intense muscular contractions activate focal adhesion kinase (FAK). Similar to insulin/IGFs, FAK activates AKT by stimulating PI-3k to convert PIP2 to PIP3. In all instances of AKT activation, the mammalian target of rapamycin (mTORC1) is activated. MTORC1 is a threonine/serine protein kinase that functions as a component in two protein complexes, mTORC1 and mTORC2, regulating cellular processes that are distinct from each other. mTORC2 regulates cell survival and cytoskeleton organization whereas mTORC1 directs biosynthetic pathways (Sciarretta et al., 2018). Activation of mTOR occurs when Rheb (RAS homolog enriched in brain), a small GTPase, binds GTP to mTORC1. Tuberous sclerosis 1/2 (TSC1/2) are upstream inhibitors of mTORC1, that are GTPase-activating proteins that encourage Rheb to hydrolyze GTP to GDP, suppressing mTORC1. When AKT is activated, TSC1/2 are inhibited allowing Rheb to act on mTORC1. The amino acids leucine is capable of activating mTORC1 independent of TSC1/2. Upon activation, mTOR phosphorylates p70s6k, a serine/threonine kinase downstream of mTOR. As the name infers, its target substrate is the S6 ribosomal protein. Phosphorylation of the S6 protein leads to the initiation of protein synthesis at the ribosomal level. S6 is able to target eukaryotic translation initiation factor- 4B (EIF4B), leading to the initiation of protein synthesis.

Muscle Protein Degradation

Forkhead box class O (FOXO) is a highly conserved family of transcription factors with important roles in cellular homeostasis (Saline et al., 2019). FOXOs respond to a variety

of stimuli including oxidative stress and nutrient deprivation. Signaling inputs regulate FOXO through many posttranslational modifications including phosphorylation, ubiquitination, and methylation. FOXO has three isoforms in muscle: FOXO1, FOXO3, and FOXO4. When phosphorylated, all three isoforms exist in the cytosol and require dephosphorylation to re-enter the nucleus. When FOXO1/3 proteins are active, they translocate to the myonuclei and act as direct transcriptional regulators of E3 ubiquitin ligases, atrogin-1 and murf-1. Ubiquitin ligases have a major effect on skeletal muscle by tagging lysine residues of proteins, targeting them to the proteasome for proteolysis. Both ubiquitin ligases are highly upregulated by FOXO3 during muscle atrophy (Bodine, 2001). FOXO transcription factors also have highly conserved phosphorylation sites that can be phosphorylated by AKT. Phosphorylation of the 14-3-3 proteins by AKT prevents the cytosolic portion of FOXO from entering the nucleus and resequesters it into the cytosol, where FOXOs can be degraded by proteasomes (Huang et al., 2005).

AMPK is a highly conserved cellular energy sensor that detects minute changes in intracellular concentration of adenosine monophosphate, a byproduct of rapid ATP turnover or energy consumption, even if ATP concentration remains relatively stable (Hardie, 2003). AMPK is capable of phosphorylating serine and threonine residues on FOXO, promoting the production of E3 ubiquitin ligases and later proteolysis. Additionally, AMPK inhibits mTORC1 by phosphorylating TSC1/TSC2 to stimulate GTPase activity upon Rheb, inhibiting mTORC1. It has also been revealed that AMPK can directly inhibit mTORC1 (Gwinn et al., 2008).

JNK: the molecular switch

c-Jun N-terminal kinase (JNK) is a member of the mitogen-activated protein kinase (MAPK) family that acts as a molecular switch between endurance exercise and resistance exercise adaptations (Lessard et al., 2018). It is activated in response to high-load contractions/mechanical tension. When active, JNK drives resistance exercise adaptations including muscle hypertrophy and satellite cell proliferation. When inactive, JNK drives endurance adaptations including mitochondrial biogenesis and angiogenesis. Activated JNK phosphorylates the linker-region of Mothers against decapentaplegic homolog 2 (SMAD2), preventing dimerization with SMAD4 and nuclear translocation. When JNK is inactive, Myostatin phosphorylates the C-terminus region of SMAD2, causing it to dimerize with SMAD4 and undergoing nuclear translocation, leading to the production of MURF-1 and MAF-bx. A dimerized SMAD2/SMAD4 also inhibits the production of muscle regulatory factors (MRFs), blunting satellite cell proliferation.

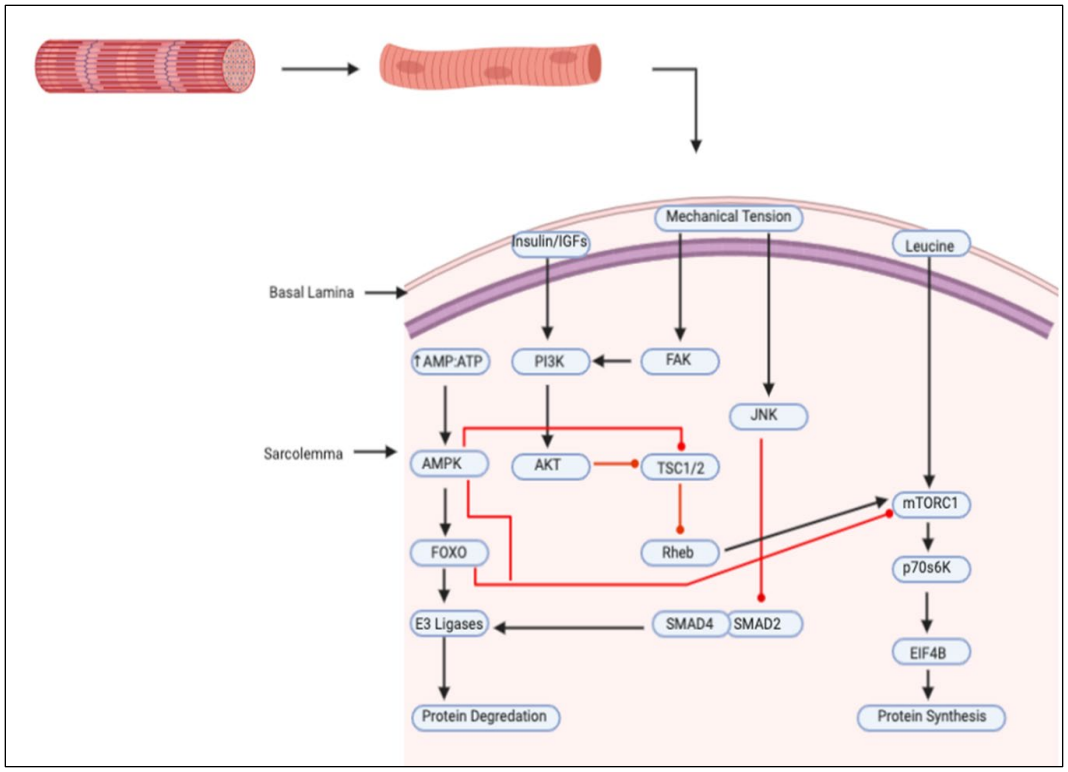

Figure 1: Visual Representation of Protein Synthesis and Degradation Pathways

Satellite Cells

Satellite cells are a form of muscle stem cells that normally reside in quiescence between the sarcolemma and basal lamina but can be activated in response to muscle damage (Snijders et al., 2015). Muscle damage leads to the activation of p38 mitogen activated protein kinase (p38MAPK). Activation of p38MAPK drives satellite cells to leave quiescence and chemotax into the muscle cell. PAX7, MYF5, MyoD all lead to the intense proliferation of satellite cells to increase their population. Myogenin is responsible for halting proliferation and initiating the differentiation of satellite cells to mature myonuclei, with MRF4 finalizing the maturation of these newly formed myonuclei. All of these newly synthesized myonuclei are now capable of producing proteins to aid in the repair of the

damaged tissue. Once the damage is repaired, satellite cells go into “self-renewal” and return to quiescence.

Satellite cells do seem to be required to support muscle hypertrophy to some extent (Fry et al., 2014), evidenced by gamma irradiation studies showing that muscle hypertrophy is almost non-existent when satellite cells are ablated (Rosenblatt & Parry, 1992; Rosenblatt & Parry, 1993). However, some controversy exists surrounding the necessity of satellite cell-mediated myonuclear accretion in supporting extensive loading-induced hypertrophy as well as the rigidity of myonuclear domain during hypertrophy (Murach et al., 2018). Extensive hypertrophy of a muscle fiber can lead to it reaching the myonuclear domain (MND) threshold- which is the largest area that a single myonuclei can regulate and maintain (Cheek, 1985). MND varies with the muscle fiber type and is inversely proportional to muscle fiber oxidative capacity (Meer et al., 2011). Beyond this threshold, additional myonuclei are believed to be donated by satellite cells to support further muscle growth via increased transcriptional capacity (Qaisar & Larsson, 2014), however, recent work by Snijders et al. (2016), reports that increases in myonuclear domain size do not appear to drive accretion of myonuclei. (Snijders et al., 2016). Thus, more research is needed to clarify this area of dispute.

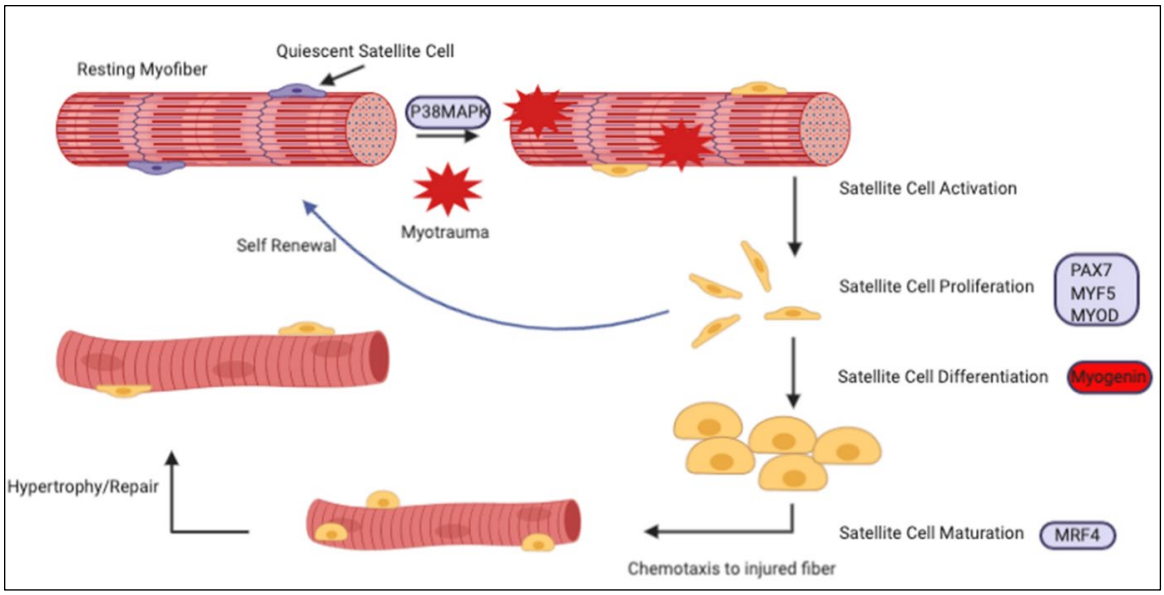

Figure 2: Visual Representation of Satellite Cell Cycle

Rationale for Usage of Animal Models

While practical outcomes of endurance and resistance exercise have largely been identified in human studies, much of the cellular and molecular mechanisms are elucidated by animal models. As previously mentioned, time to exhibit adaptations and ethical concerns limit the quantity of data that can be obtained. The adaptations to resistance exercise are ubiquitous and animal models have the benefit of easily being able to collect whole tissues throughout the body after euthanasia such as the brain, liver, heart, and skeletal muscle, which could not be collected from human subjects (Cholewa et al., 2014). In contrast, various rodent models have been reported to induce rapid and extensive muscle hypertrophy and some models allow precise control of the diet and exercise parameters (Cholewa et al., 2014). Additionally, in humans, a Bergström muscle biopsy removes only 100-200mg of muscle tissue (Shanely et al., 2014), which may not be as representative of cellular signaling/protein content as the whole muscle tissue that can be excised from rodents.

Rodent Models of Involuntary Skeletal Muscle Hypertrophy

One of the first rodent models of involuntary skeletal muscle hypertrophy tested was **synergistic ablation** (Goldberg, 1968). The Achilles tendon was surgically altered, severing the connection of the Achilles tendon from the gastrocnemius (GAS) on one side. This resulted in significant compensatory hypertrophy in the soleus (SOL) and plantaris (PLT) muscles, as the workload on the remaining ankle extensors was increased significantly. Within five days, the mass of the SOL increased by 36% and the mass of the PLT increased by 15%. However, after five days there was no further increase in muscle mass due to the tendon reattaching. This complication was later resolved by completely removing the GAS and SOL, which resulted in a 65% increase in PLT mass after 12 weeks of ablation (Baldwin et al., 1982). The increase in muscle mass was also directly proportional to the increase in amino acid incorporation. The percentage of water did not change in muscles during hypertrophy, indicating that the increase in muscle mass was not due to edema. The surgical procedure can also be modified to ablate synergists to varying degrees (Nakada et al., 2016). For example, Nakada et al., (2016) performed four ablation surgeries characterized as weak, moderate, middle, and strong. Weak ablation removed approximately half of the GAS, moderate and middle ablation removed portions of the GAS and the entire SOL, and strong ablation removed the entire GAS and SOL. Both mass and fCSA of the PLT increased proportionally to the degree of synergist ablation. Additionally, total rpS6 increased with degree of ablation and rRNA content was strongly correlated with rpS6 content. This model has received great criticism due to the surgical procedures (Taylor & Wilkinson, 1986). Following surgery there is risk of infection and massive inflammation warrants that results measured within one-week be evaluated with caution. Despite the criticisms, synergistic

ablation remains a viable option to study cellular signaling pathways leading to skeletal muscle hypertrophy because of the large magnitude of hypertrophy (Miyazaki & Esser, 2009).

Wong & Booth (1988) developed a rat model that consisted of **electrically stimulating** the lower leg to contract against a weighted pulley. Training loads started at 200g and progressively increased to 800g over a 16-week period. Work (Joules) done at the end of the training period increased by 66% compared to the start of training. GAS wet mass and protein content increased by 18% and 17% respectively in the stimulated leg, with a concomitant increase in RNA content. This combination of stretch and electrical stimulation induced the activation of an IGF-1 derived transcript called mechano growth factor (MGF), which results in satellite cell proliferation and activation following muscle damage, leading to muscle repair and hypertrophy (Hill & Goldspink, 2003). Although the combination of muscle lengthening and involuntary contractions may be viable to study acute increases in protein synthesis, the ability to provide a consistent overload in electrical stimulation to emulate an increased load to induce hypertrophy is incredibly difficult to do under anesthesia.

Similar to the previous model, Baar & Esser (1999) utilized the surgical implantation of electrodes and electrical stimulation of the sciatic nerve. The electrodes were implanted above the point of trifurcation of the sciatic nerve so all muscles were stimulated simultaneously. Muscle contractions were generated by stimulating the nerve at 100hz with the frequency sufficient to stimulate both slow and fast-twitch motor units. The voltage was adjusted to provide maximal contractile force. Over the course of a 22-minute period, 10 sets of 6 contractions each 3-seconds in duration were provided. This resulted in a net

plantarflexion because plantar flexors (GAS, SOL, PLT) produce more force than dorsiflexors: tibialis anterior (TA) and extensor digitorum longus (EDL) (Wong & Booth, 1988). The net ankle plantarflexion results in an eccentric muscle contraction for dorsiflexors and a concentric contraction for plantar flexors. This resulted in an increased wet mass of 14% in both the TA and EDL, with no change in protein concentration. There were no significant changes in SOL or PLT wet mass. A potential criticism of this model is that significant hypertrophy was only exhibited in muscles that were eccentrically contracted, which are able to produce more force per unit of cross-sectional area than a concentric contraction (Wilkie, 1949). This indicates that there may only be sufficient stimulus to provide hypertrophy in ankle dorsiflexors.

Weighted ladder climbing has been utilized as a rodent model of involuntary skeletal muscle hypertrophy. Weighted ladder-climbing consists of masses of known weights being tied to the tail of rats and the animal climbing up a steep ladder mesh. This model requires the animal to be conscious for exercise and thus, operant conditioning must occur. To condition the animal, encouragement to climb up a steep ladder with a small amount of food as a reward is provided. Operant conditioning can take several sessions to accomplish, and even when fully conditioned, a researcher must be present to ensure the animal performs the proper amount of exercise. Yarasheski et al. (1990) first trained ten Long Evans rats to lift progressively heavier weights, while they climbed up a 40cm ladder 20 times per day, 5 times per week. Every five days the load tied to the animal's tail increased by 30g, and after eight weeks of training, the average mass animals lifted was 406g. In comparison to sedentary controls, trained animals displayed no difference in forelimb muscle mass but rectus femoris (RF) wet and dry weight was increased ($p<0.01$). However, increases in fiber

area were limited to the superficial region of the RF, which is dominated by fast-IIB fibers. Later, Duncan et al. (1998) trained Wistar rats to climb a 40cm ladder, 4 days per week for 26 weeks, after which animals were capable of lifting 800g or 140% of their body mass for 4 sets of 12-15 repetitions (one climb) per session. When expressed in relative muscle mass, the mass of the EDL, SOL, and RF was greater in the trained group than the sedentary group. Despite the increase in ability to lift progressively heavier loads up the ladder, there were no changes in absolute muscle mass, fiber type proportions, or force-producing capabilities. Lee et al. (2004) used a 100cm ladder with an 85-degree incline with more success. The eight-week protocol used Sprague-Dawley rats and started with a load of 50% of body mass. If the animal was able to climb the ladder with 50,75,90, and 100% of the loads from the previous session 30g would be added each climb until the animal failed to climb the entire length of the ladder. Electrical shock of 0.2-0.3mA was used to provide motivation if necessary and training was stopped when three shocks were insufficient. The protocol resulted in a 23.3% increase in mass of the flexor hallucis longus (FHL) and an increase of *in situ* peak tetanic force of 14%.

With similar success, Hornberger & Farrar (2004) trained Sprague-Dawley rats with a 110cm ladder with an 80-degree incline every three days for 8 weeks, each session consisting of 4-9 climbs requiring 8-12 dynamic movements per climb - similar to human models of resistance training. They reported a 287% increase in carrying capacity, 23% increase in FHL absolute mass, and a 24% increase in total myofibrillar protein content with Sprague-Dawley rats.

It is evident that weighted ladder climbing provides positive adaptations, but minor protocol modifications can greatly influence results. The differences in results between these

models could be related to the muscles sampled, overload progression, volume in protocols, and number of sessions per week. Sampling of muscles that consist of predominantly type II fibers, such as GAS and PLT, may provide more insight into the effectiveness of this model. Additionally, the requirement of operant conditioning and the periodic use of electrical shock may introduce stress as a confounding variable in influencing training adaptations.

Tamaki et al. (1992) employed a canvassed squatting model. Hypertrophy in the hind-limb muscles was induced by loading the animal, rats in this instance, with a canvas-like jacket attached to the torso and requiring the animal to perform a squat-like movement. An electrical stimulus was provided by a surface electrode linked to the tail of the animal and as a result, the rats extended their legs. Fifteen sets of fifteen reps were performed at 65-75% of the rats predetermined 1RM squat, with 1RM being reassessed every two weeks. After twelve weeks of progressively increasing load, the PLT and GAS in the squat-training group exhibited a 31.4% and a 17.9% greater normalized mass compared to control animals. SOL and EDL muscles were not significantly hypertrophied. The total number of muscle fibers was also 14% greater than the control group. A benefit of this model is that the loading pattern is similar to the squat exercise in human resistance training but its ability to apply overload is inferior to other involuntary models as it relies on an electrical stimulus to induce movement.

Wirth et al. (2003) developed a rat model that relies on both operant conditioning and reward to perform a squat in a tube. Initially, food was restricted to 80% of their ad libitum diet, and rats were operantly conditioned with food rewards to enter a vertical tube. Then the animal would insert its head into a weighted ring, either 70g or 700g, and lift the ring until the nose was detected by an infrared sensor, again with food as a reward. Rats were able to

successfully perform this movement after 12-15 practice sessions, practicing 5 days per week. After conditioning, additional training sessions were performed until the number of lifts (nose detections) was consistent. For most rats, the number of lifts stabilized after 20 sessions. Each session ended after 100 successful nose detections. Although analysis of hypertrophic responses was not measured in this study, preliminary data from a separate study by this lab showed that as little as eight weeks of training resulted in a significant increase in wet mass of plantar flexor muscles (GAS, PLT, and SOL). Unfortunately, food only functions as a reward if the animal is hungry. If the animal is kept in a slightly underfed state, that may not be an optimal condition to measure hypertrophic outcomes.

One model that does rely on a voluntary rodent behavior, feeding, has shown to be an effective model at promoting muscle adaptations and upregulation of the mTOR pathway (Cui et al., 2020). This model also only requires a short, two-day acclimation period. Simply, the regular cage top was replaced with a modified weightlifting cage top during the dark cycle to eliminate the need for human handling. The weightlifting cage top had a long lever plate with masses attached to the end, starting at 100% of mouse body mass and plateauing at 240% of body mass. In order to feed and access food, the mice in the exercise group wore a neck collar and needed to walk up a short ramp and push its head through a hole in and lift up the weight-loaded lever plate with the load supported on its shoulders, extending its hindlimbs to perform a squat-like movement. This motion was performed an average of 419±82 times per night and did not have any adverse impact on body mass. After eight weeks of training five times per week, there was a 14% increase in CSA of plantar flexor muscles (GPS complex, measured by MRI) and a modest increase in GAS, PLT, and SOL wet mass of 8-12%. They also performed a non-invasive contractile function assay on the

plantar flexor muscles in the hindlimb via *in vivo* sciatic nerve stimulation and displayed a 35% and 20% increase in twitch and peak tetanic torque, respectively. There was no increase in heart mass or changes to cardiac function, which is consistent with human resistance exercise training regimens.

More recently, a model that involves **weighted pulling** was developed that induced robust skeletal muscle hypertrophy (Zhu et al, 2021). This weighted pulling model consisted of attaching an unweighted or weighted cart to the base of the tail of the mouse. The initial training sessions to assess "one repetition max" ended when mice could not pull the cart- loaded with dozens of times their body mass- along the 50cm long track. After the familiarization period, each training sessions, performed three times per week for twelve weeks, consisted of a warm-up set with an empty cart, and then 50, 75, 85, 90, 95, and 100% of the mouse's previous pulling maximum along a grippy 50cm long track with two minutes rest between sets. Following, an additional 15 grams would be added until the mouse could not pull the cart without need for touch of shock inventive. The average training session consisted of 10-12 sets. To pull the cart the length of the track, the mice generally needed to engage in 8-12 vigorous contractions- a commonly prescribed repetition range for hypertrophy. Twelve weeks of weighted pulling resulted in an 18% increase in average PLT fCSA. Additionally, it led to an 6-23% increase in wet mass of 10 of the 15 different skeletal muscles that were harvested: hind limbs, forelimbs, and torso. There was also a 42% increase in isometric grip strength. On a molecular level, an acute bout of weighted pulling increased the phosphorylation of MAPKs, downstream markers of mTORC1 activity, and increased the rate of protein synthesis. The latter is measured by update of puromycin-labels peptides.

It is evident that all of these models, if done correctly, can be effective models of skeletal muscle hypertrophy. However, a primary downfall of these models is that they are entirely involuntary, are not part of normal rodent behavior, are time-intensive, and invasive. Further, these models often induce a hypertrophic response that is so robust that it is not in line with the magnitude and timescale of normal human skeletal muscle hypertrophy.

Voluntary Wheel Running in Rodents

Many mouse and rat strains voluntarily run long distances when given access to a free running wheel, and do not rely on positive/negative reinforcement or anesthesia to force movement (De Bono et al., 2006; Goh & Ladiges, 2015). Meijer & Robbers (2014) report when a running wheel is placed in nature, with no extrinsic reward, wild mice frequently use the running wheel. This wheel running has a voluntary component not a result of being captive. Wheel running occurs with routine diurnal patterns in the laboratory setting and does not exhibit stress in a laboratory setting (Goh & Ladiges, 2015). Running activity depends greatly on mouse strain, sex, age, and an individual basis. Lightfoot et al. (2004) compared the running activity of 15 different mouse strains and found that daily running distance ranges from 2.93km to 7.93km, with C57BL/6J mice running the farthest regardless of sex. Similarly, Lerman et al. (2002) found that daily running distance ranges from 1.4km to 7.6km, with C57BL/6J mice running the farthest.

Lightfoot et al. (2004) also reported that female mice ran 20% further than male mice. Although male mice were heavier on average, there was not a significant association between body mass and daily running distance. The strongest sex-related effect was related to running speed as overall, females ran 38% faster than males. It is also well accepted that regardless of strain or sex, older mice will run less compared to younger mice (Manzanares et al., 2018).

Upon examining the literature, there are no studies explicitly investigating the effect of rat strain on running activity; however, several studies have included free wheel running as part of their study design. Kurosaka et al. (2009) found that male Wistar rats ran an average of 6.6km per day. Ishihara et al. (1998) and Legerlotz et al. (2008) found that Sprague-Dawley rats ran 2.3km and 1.3km, respectively. Sexton et al. (1995) reported that Sprague-Dawley rats run an average of 4.1km per day but individual animal activity varies greatly from 0.6km to 10.6km per day.

Muscle Hypertrophy in Free Wheel Running Models

As stated above, FWR is a voluntary activity and daily running distance ranges from 1.4km to 7.93km per day. FWR is commonly accepted as an excellent model for inducing endurance and cardiac adaptations (Allen et al., 2001; Ishihara et al., 1998; Kurosaka et al., 2009; Lambert & Noakes, 1990; Rodnick et al., 1989; Sexton, 1995), although its effectiveness at inducing skeletal muscle hypertrophy is less conclusive as few studies yield significant increases in limb muscle mass. Using C57BL/6J mice, Allen et al. (2001) reported that four weeks of FWR elicited no differences in mass of TA, GAS, or PLT. This particular group of mice (n=4) ran an average of 6.8±2.6 km per day. Lerman et al. (2002) observed a comparable running distance of 7-8km per day but no significant changes in muscle mass or function. Call et al. (2010), using C57BL/10ScSn-DMDmdx, found that while absolute muscle mass did not differ between the FWR group and sedentary mice, relative mass of the SOL and TA muscles in the were 23% and 15% greater than sedentary mice. A limitation of these data sets is that the mouse strain used has characteristics of Duchenne muscular dystrophy: muscle weakness and susceptibility to injury. A potential explanation of the

differences in muscle mass is that the FWR group maintained muscle mass and function, whereas the sedentary group continued to decline.

Ishihara et al. (1998) measured PLT hypertrophy of 5-week-old Sprague-Dawley rats in response to seven weeks of FWR. They reported that following acclimation animals ran 2-2.5km/day and did not exhibit significant PLT hypertrophy compared to sedentary animals. Kurosaka et al. (2009) reported similar results- no significant hypertrophy of the PLT took place following eight weeks of FWR. Conversely, Legerlotz et al. (2008) reported that Sprague-Dawley rats that engaged in six weeks of FWR had a SOL 27% greater in relative mass than sedentary animals. Munoz et al. (1994) report that within one week of FWR, SOL wet weight and protein content had increased, while it took two weeks to see an increase in MPS and it took two weeks to see an increase in those parameters in the PLT. Overall, these studies indicate that FWR is not a reliable model to induce skeletal muscle hypertrophy, especially in mice.

Muscle Hypertrophy in Responses to Loaded Wheel Running

The hypertrophic effect of wheel running might be augmented by increasing resistance of the running wheel. Additional resistance has been applied most commonly by adding a calibration mass to the moment arm of the wheel, and then a magnetic brake or a bolt will be tightened until the wheel will no longer spin with the mass, after which the mass is removed. Alternative methods involve securing magnets of a known mass to the circumference of the wheel in an asymmetrical fashion (Dungan et al., 2019). After allowing the rodents time to acclimate to the unloaded wheel, the resistance is progressively increased over several weeks, with varying rates of progression. In rats, eight weeks of loaded wheel running (LWR) with a progressively applied load up to 74% of body mass led to a 19%

increase in absolute PLT mass (Ishihara et al., 1998). A strong correlation (r=0.85) existed between muscle weight and total work. Six weeks of LWR starting with a load of 93% body mass and progressively increased to 173% body mass, resulted in a greater relative muscle mass for the SOL, PLT, VL, extensor carpi radialis longus and brevis by 23%, 29%, 17%, and 21% respectively compared to sedentary rats (Legerlotz et al., 2008).

Additionally, in response to 6 weeks of LWR up to 60% resistance, relative GAS and PLT mass were 13% and 16% greater respectively in exercised rats than sedentary rats (Mobley et al., 2018a). In adult ICR mice, a load progressively increased up to ~33% of body mass did not result in an increased TA mass after four weeks of training (Ishihara et al., 2002). Soffe et al. (2016) placed C57BL/6J mice into a sedentary, low load (up to 13% of body mass), or high load group (up to 20% of body mass). After twelve weeks of exercise, SOL and quadriceps were larger in the low load and high low group than the sedentary group but neither exercise group outperformed the other. Also placed into sedentary, low load (up to 17% of body mass or 5g), and high load (up to 41% of body mass or 12g) groups, eight weeks of exercise did not elicit an absolute increase in SOL, TA, PLT, or GAS mass, but a 20% increase in relative SOL mass for both high load and low load groups were observed (Konhilas et al., 2005). Additionally, in C57BL/6J mice, an acute (24 hour) exposure to LWR with 60% resistance resulted in significantly greater downstream mTORC1 signaling in the SOL and PLT than FWR and sedentary mice (D'Hulst et al., 2019). The same lab group has also demonstrated that long-term LWR with their model, with 50-74% resistance resulted in an increased SOL mass of ~20% and an increase in SOL and PLT fCSA, whereas increased muscle mass was not observed in FWR group (Masschelein et al., 2020). The authors also observed a significant accumulation of satellite cells in the GAS, PLT, SOL, and

EDL that was greater in response to LWR than FWR, indicating that satellite cell activation might be load-dependent, though does not necessarily correlate to muscle hypertrophy. Recently, a progressive weighted wheel running model named "PoWeR" was developed that involves the asymmetrical loading of magnets on the running wheel. As opposed to running wheels with constant resistance that encourages constant running, the asymmetrical loading encourages shorter repeated bouts of running- more akin to traditional resistance exercise (Dungan et al., 2019). Utilizing the PoWeR model, adult female mice will run 10-12 km per night with 6g on the wheel while adult males run slightly less. Both the PLT and SOL grow 15-30% in whole muscle and fCSA, with a significant shift in glycolytic to oxidative fiber type shift and myonuclear accretion. The authors acknowledged that PoWeR is not exclusively hypertrophic due to the high volumes of running- a phenomena that is not exclusive to PoWeR but other LWR models as well- and should be used knowing that it is a combination of endurance and resistance exercise (Murach et al., 2020).

In review, LWR displays greater effectiveness at inducing skeletal muscle than FWR. The LWR model in rats has a tendency of using a higher resistance than mice, 40-173% of body mass versus 5-60% of body mass, and this discrepancy may contribute to the less pronounced hypertrophy exhibited in mice. Regardless, as mouse handling and stress is minimal, LWR is an excellent model of exercise training that provides similar muscular adaptations as other well-accepted models. Additionally, since there is minimal direct intervention from researchers and entire cohorts of mice can be trained simultaneously, it can easily be employed in long-term studies (i.e., 6 to 12 months).

This model is not immune to limitations: namely, the large and highly variable running volumes between individual animals. To start, adding resistance to a running wheel

would be expected to alter running patterns, primarily a decrease in running distance. Several studies in rodents confirm this expectation, showing that the LWR model decreases daily running distance, especially as resistance continues to increase (Call et al., 2010; Mobley et al., 2018a; Soffe et al., 2016). However, the degree to which resistance deters running varies. Moreover, several studies show that LWR does not significantly decrease running distance (D'Hulst et al., 2019; Ishihara et al., 2002; Legerlotz et al., 2008). The variation is potentially due to differences in LWR protocol: duration of study, load, load application strategy, and rodent strain, sex, and age. As such, the maximum loads at which rodents will severely discontinue use of the running wheels have not been elucidated. If running distance is not sufficiently deterred by wheel load, excessive running distance may be more reflective of concurrent training as opposed to strictly resistance exercise. This concern was also acknowledged in the mini-review "Making Mice Mighty: recent advances in translational models of load-induced muscle hypertrophy" (Murach et al., 2020). While the full effects of concurrent training are not fully elucidated, it could diminish the potential for muscle hypertrophy and strength by introducing the interfering effects of endurance training adaptations and concomitant upregulation of protein degradation pathways. Thus, ensuring that a concurrent training phenomenon is minimized in what is intended to be a resistance exercise model is imperative. That said, the limitation of high and variable running volumes due to increased wheel resistance can be used to determine if there is a dose-response relationship between running volumes and hypertrophy so long as LWR protocol is consistent.

Table 1: Summary of Previous Wheel Running Studies

Author	Species	Duration	Wheel Resistance	Running Distance	Hypertrophy
Allen (2001)	Mouse	4wk	FWR	6.8km	GAS, PLT, TA: None
Lerman (2002)	Mouse	2wk	FWR	8.0km	GAS, PLT, SOL: None
Call (2010)	Mouse	12wk	FWR	6.7km	SOL: +23% TA:+15%
Ishihara (1998)	Rat	7wk	FWR	2-2.5km	PLT: None
Kurosaka (2009)	Rat	8wk	FWR	6.6km	PLT: None
Legerlotz (2008)	Rat	6wk	FWR	FWR: 1.2Km	SOL: +27%
Ishihara (1998)	Rat	8wk	LWR, 74%	0.5-2.5km	PLT: +19%
Legerlotz (2008)	Rat	6wk	LWR, 93-173%	1.4km	SOL: +23% PLT: +29% VL: +17% ECRl/b: +21%
Mobley (2017)	Rat	6wk	LR, 60%	Not Mentioned	GAS: +13% PLT: +16%
Ishihara (2002)	Mouse	4wk	LWR, 33%	.84-1.06km	TA: None
Soffe (2015)	Mouse	12wk	LWR: 13% LWR: 20%	0.9- 9.75km	SOL: +25% QUAD: +15%
Konhilas (2015)	Mouse	8wk	LWR: 17% LWR: 41%	LWR: 4km LWR: 0.5-3km	SOL: +20% rel
Dungan (2019)	Mouse	9wk	LWR: 6g	12km	PLT/SOL: 15-30%
White (2016)	Mouse	34wk	6g	2-4km	QUAD: +11% GAS: +7% SOL: +46% EDL: +16%

Chapter 3. Methods

Animals

Male C57BL/6 mice procured from the in-house colony at Appalachian State University were randomly assigned to one of four groups (n=6-12 each): sedentary (SED), free wheel running (FWR), standard loaded wheel running (LWR), and high LWR (HLWR). Mice were 12-24 weeks of age at the start of the study as daily running activity plateaus around 9-10 weeks of age (Swallow et al., 1998). All mice were individually housed in a cage with a running wheel and kept in a controlled environment with a 12:12-hour light: dark cycle. Standard rodent chow and water was available *ad libitum* and food consumption was measured daily. This study was approved by the Appalachian State University IACUC (#22-05).

Running Wheel Apparatus and Loading Protocol

All mice had free access to a running wheel that is 11.4cm in diameter with an 8cm wide running surface (Kaytee Silent Spinner Exercise Wheel, PETCO, Inc.). Each cage was equipped with a digital bike computer (Sigma Sport, BC 509) to monitor time exercising, distance traveled (set at 0.358 m/revolution), and average speed (km/hr). The bike computer was observed daily at a consistent time interval to record all data. A small magnet adhered to the middle circumference of the wheel functioned as a sensor for the bike computer to detect each wheel revolution (Figure 3).

The entire protocol was conducted over a 9-week period. For mice in the FWR, LWR, and HLWR groups, week 1 consisted of an acclimation phase to allow the mice to become accustomed to running on the wheel with no load (i.e. free wheel). If mice did not show an inclination to run within the acclimation week (<1 km/day), they were placed into

the SED group. Mice in the FWR group continued to have access to a running wheel for the 9-week protocol, but no load was applied to the wheel. Starting on week 2, mice in the LWR and HLWR groups began their respective progressive 8-week wheel loading protocols. Wheel loading was applied by adhering loading magnets to the outer circumference of the running wheel, where additional loading magnets were stacked to apply more load (Figure 3).

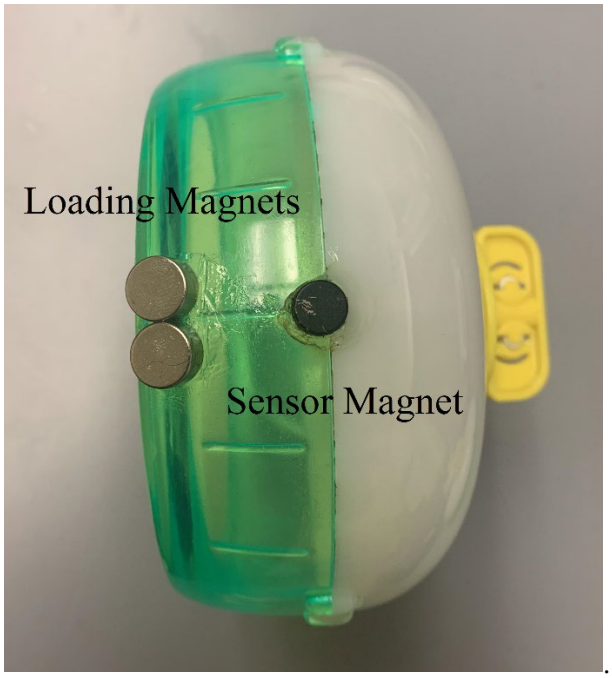

Figure 3: Running wheel magnet application. The sensor is glued to the middle circumference of the wheel and passes under the bike computer sensor each revolution, recording running distance and velocity. The loading magnets are glued to the outer circumference of the wheel to apply the external load.

The progressive loading protocol for the LWR group is identical to that of the PoWeR model established by Dungan et al. (Table 2) and was used as a treatment comparison group (Dungan et al., 2019). Whereas the loading protocol that was used for the HLWR group was developed using information gathered from a pilot study with mice of the same strain and age

(Table 3). Wheel load in relation to body mass is based on C57BL/6 body mass data provided by The Jackson Laboratory comprehensive database. Additionally, to ensure mice continued to exercise, load was reduced to that of the previous week if running distance dropped below 250 m over a 24-hour period. Mice in the SED group had a running wheel in their cage, but it was locked to prevent running during the entire 9-week protocol.

Table 2: LWR loading protocol

Week	1	2	3	4	5	6	7	8	9
Load (g)	0	2	3	4	5	5	6	6	6
% BM	0%	9%	13%	17%	22%	22%	26%	26%	26%

Table 3: HLWR loading protocol

Week	1	2	3	4	5	6	7	8	9
Load (g)	0	2.5	5	7.5	7.5	10	10	12.5	12.5
% BM	0%	11%	22%	33%	33%	43%	43%	54%	54%

Load progression in the LWR protocol is identical to that used in the PoWeR model as a treatment comparison group, Dungan et al., 2019. Percent (%) body mass (BM) is the result of added load divided by animal body mass.

Isometric Forelimb Grip Strength Test

At the beginning of the 9-week protocol, as well as weekly throughout the 9-week protocol, body mass and grip strength were recorded for each mouse. The grip strength procedure was performed three times and the maximum was taken. The procedure was repeated on a weekly basis until the conclusion of the 9-week protocol, where mice underwent a final forelimb grip strength test. The grip strength procedure is a simple and non-invasive method to assess muscle strength in live, un-anaesthetized rodents (Castro & Kuang, 2017). After weighing the mouse, it was grasped by the base of the tail and then

allowed to grab the wire bar attached to the grip strength device with their forepaws. Keeping the torso parallel with the bar, the mouse was slowly and gently pulled by the base of the tail backwards, away from the bar in a linear direction, until their grip failed (Figure 4).

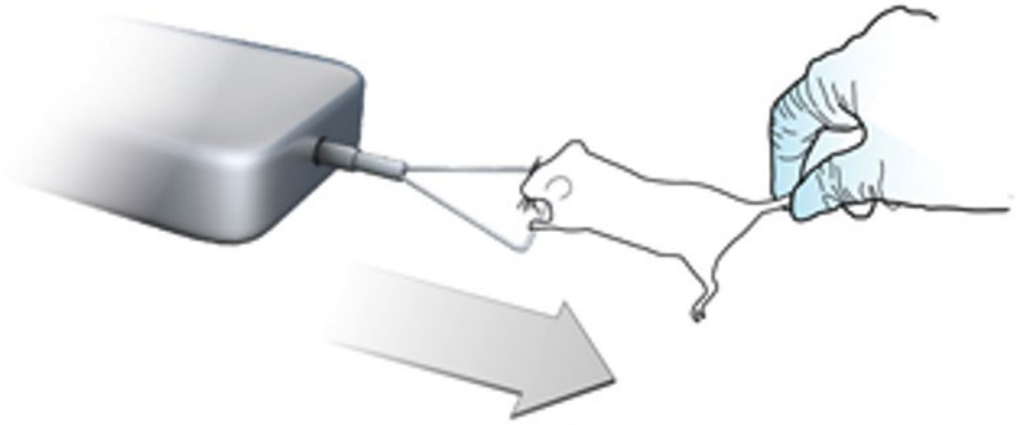

Figure 4. Demonstration of the grip strength test for muscle strength, using the forelimbs

The grip strength device (Columbus Instruments; 1027SM Grip Strength Meter; Figure 5) measures the maximal force exerted by the mouse's grip and this value is recorded as grip strength. The procedure was repeated two more times, for a total of three measurements for each mouse, and the maximal value was used for data analysis.

Figure 5. Grip strength device (Columbus Instruments; 1027SM Grip Strength Meter)

In Situ Contractile Function

Following the final forelimb grip strength test at the end of the 9-week protocol, the *in situ* contractile function procedure was performed to determine strength of the posterior plantar flexor muscles of the hindlimb for each mouse according to previously published methods (Mackay et al., 2021). First, the animal was deeply anesthetized with 4% isoflurane and anesthesia was maintained with 2% isoflurane for the duration of the procedure. The mouse was then placed on a heated platform to maintain body temperature. Using only the right limb, the hamstring muscle and excess tissue was dissected away to expose the sciatic nerve and to isolate the gastrocnemius, plantaris, soleus (GPS) muscle complex (aka, the posterior plantar flexor muscles). The distal Achilles tendon and the GPS complex of the

right limb was then released up to its proximal origin to mitigate any lateral transmission of force from nearby muscles. This procedure leaves all innervation and vasculature to the GPS complex intact. To prevent movement of the knee joint, the patella tendon was secured to a vertical post on the heated platform via 2-0 surgical suture.

The Achilles tendon, with a part of the calcaneus bone still attached to alleviate slipping, was then secured to a 4 cm lever arm connected to the servomotor of the Aurora Scientific 1305 Muscle Testing System via 2-0 suture (Aurora Scientific, Toronto, ON, Canada). Two microelectrode needles were placed superficially staggering the sciatic nerve. Electrode placement was optimized using single electrical pulses (10mA) to produce muscle contractions of the GPS complex. Resting muscle length was adjusted very carefully until resting tension reached 0.1N (Weber et al., 2012). Following optimal muscle length and stimulation amplitude, measurement of isometric muscle strength of the GPS complex was performed using a force-frequency curve with 11 ascending stimulation frequencies ranging from 1 Hz to 300 Hz, with two minutes rest between each contraction. The force-frequency curve is designed to assess muscle strength from submaximal, unfused, tetanic, contractions up to maximal, fused tetanic contractions, with maximal fused tetanic contractions typically observed between 100-200 Hz. This specific force-frequency curve was published by Ingalls et al. (2014) and has been successfully conducted in our lab in previous experiments (Godwin et al., 2020; Zwetsloot et al., 2021).

Tissue Collection

Immediately following the *in situ* contractile function procedures, mice were euthanized, and tissues harvested. For histological purposes, the gastrocnemius, plantaris, soleus, and triceps muscles from the left limb were excised and cleared of excess connective

tissue, then tissue mass recorded, and tissues were individually preserved for histological analyses. Each histological muscle sample was coated in an embedding medium (Tissue-Tek OCT; Miles; Naperville, IL, USA), mounted on cork, cryopreserved in liquid nitrogen-cooled isopentane, and stored at -80℃ until further use. For future cell signaling analyses, the gastrocnemius, plantaris, soleus, and triceps muscles from the right limb, and the quadriceps muscles from both limbs (separated into predominantly white and predominantly red portions), as well as the heart were excised, then flash frozen in liquid nitrogen and stored at -80℃ until further use.

Histology and Immunohistochemistry

Muscle tissues were sectioned transversely (10 μm thick) at -16℃ using a cryostat (Cryostar NX50, Thermo Fisher Scientific, Waltham, MA) placed on charged slides, and then stored at -20℃. Immunohistochemistry (IHC) against the extracellular matrix protein, laminin, was performed to detect the muscle fiber membrane. Briefly, slides were removed from the freezer and allowed to warm to room temperature. The tissue sections were encircled using a hydrophobic-barrier PAP Pen (Vector, ImmEdge pen, Cat # H-4000). Tissue sections were blocked by incubating with approximately 50 microliters of 10% normal goat serum (NGS; Vector, S-1000) in 1X phosphate-buffered saline (PBS) at room temperature for one hour. Blocking buffer was carefully removed via aspiration. Tissues were incubated overnight at 4°C with 1:200 laminin primary antibody, conjugated with an AlexaFluor (AF) 547 fluorophore (Novus Biologicals, NB300-144AF647. After incubation, primary antibodies were removed via aspiration and PAP pen ring was reapplied, if needed. Tissues were washed for three rounds of five minutes with approximately 50 microliters of 0.04% Triton X-100 in 1X PBS (wash buffer). After fully air drying, coverslips were applied

using Vectashield® Vibrance with DAPI (Vector, H-1500) to stain all nuclei. All tissue sections were imaged using fluorescence microscopy (EVOS® FL Imaging System, Life Technologies, Carlsbad, CA). Images of the sections were digitized and fiber cross-sectional area (fCSA) was determined using the semi-automated software program, Myovision (Wen et al., 2018). Average fCSA and minimum feret diameter was reported. Minimum feret diameter is defined as the closest distance between two parallel tangents of an object and is utilized because the measurement is less susceptible to the inclusion of longitudinal fibers (Pertl et al., 2013).

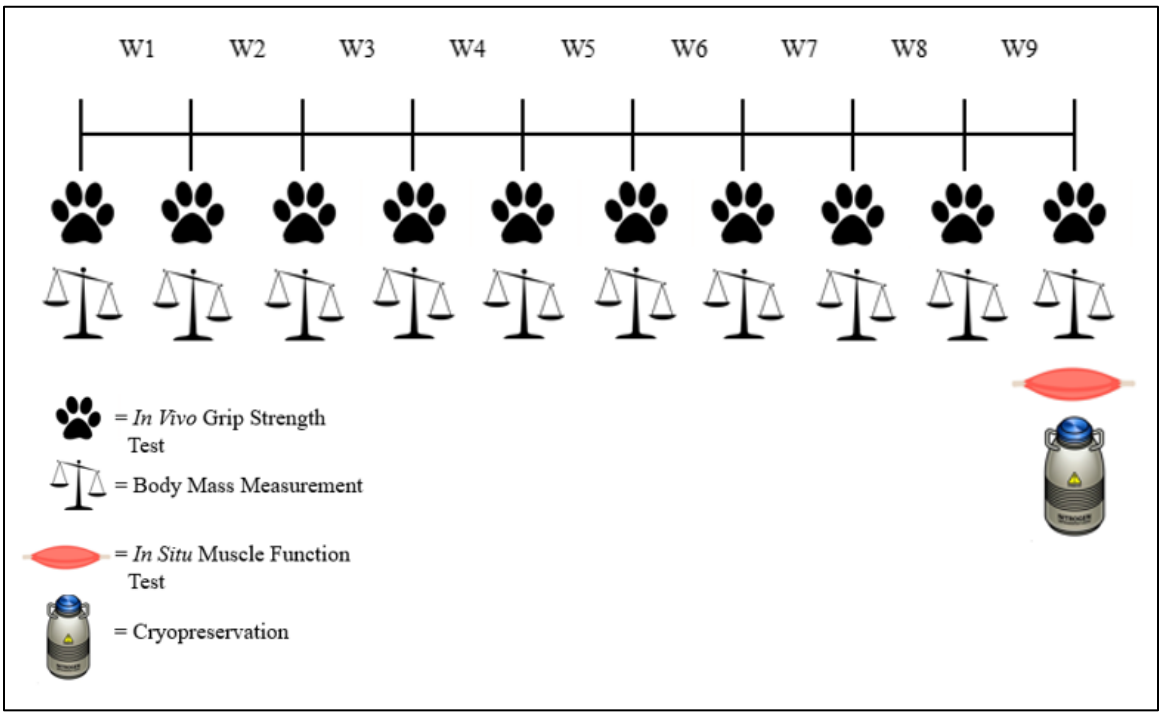

Figure 6. Schematic of procedures performed throughout the 9-week training protocol. Grip strength and body mass were performed at baseline and weekly thereafter until the conclusion of the 9-week training protocol. At the end of the 9-week protocol, the final grip strength and body mass measurement were performed, and then the in situ muscle function test, tissue harvesting, and cryopreservation were performed.

Statistics

Data were analyzed using SPSS (IBM SPSS Inc., Version 28.0.0.0., Chicago, IL, USA). One-way ANOVA was used for food consumption, muscle mass, muscle strength, mean fiber cross-sectional area, and minimum feret diameter for comparisons between groups. Weekly averages of body mass, running distance, duration, and speed for each group were analyzed with repeated measures two-way ANOVA. Following a significant F-ratio, Fisher's LSD *post hoc* analysis was performed. Significance was set *a priori* at $p<0.05$. Data are expressed as mean ± SD.

Chapter 4. Results

Animal Characteristics

Thirty-four male mice aged 6.3±0.8 months were randomly assigned to one of four experimental groups: sedentary (SED), free wheel running (FWR), loaded wheel running (LWR), and high loaded wheel running (HLWR). All mice that did not show an inclination to run (<1 km/day) within the first week were placed into the SED group. At the end of the 9-week training protocol, all mice that did not run an average of 2 km/day between weeks two and three were culled from the data set and consequently removed from all statistical analyses, as they likely did not receive sufficient training stimulus to elicit muscular adaptations. Following culling, twenty-eight mice remained with experimental group populations as follows: SED (n=13), FWR (n=4), LWR (n=4), HLWR (n=7). Average body mass of all mice at the start of training was 26.5±2.4 grams with no differences between groups (Figure 7). There was a significant main effect of time on body mass, as body mass significantly increased by ~1 gram ($p<0.001$) over the 9-week protocol; however, there were no differences were observed between treatment groups ($p=0.453$). Overall, average daily food intake increased significantly ($F=10.451$, $p<0.001$) by 18.5% in all wheel running groups compared to SED mice, but no post hoc differences were observed between running wheel groups (Figure 8).

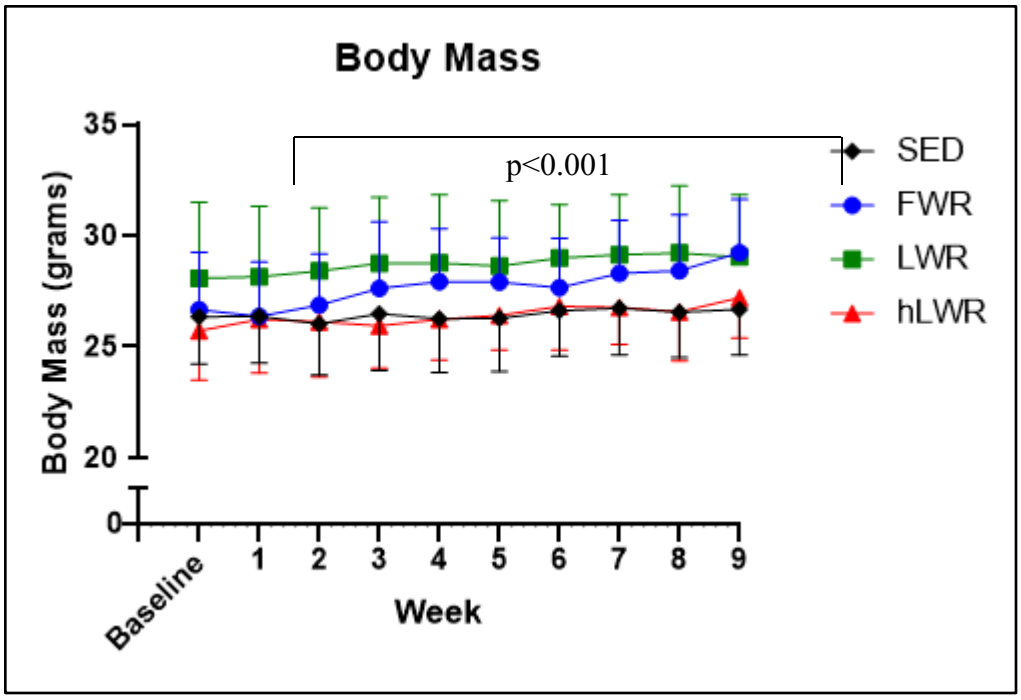

Figure 7. Body mass over the 9-week protocol. Body mass was recorded on a weekly basis for all mice throughout the 9-week protocol. There was a significant main effect of time as body mass increased approximately 1 g overall by the end of the 9-week protocol; however, there was no effect of treatment with regards to body mass. Data are expressed as mean ± SD.

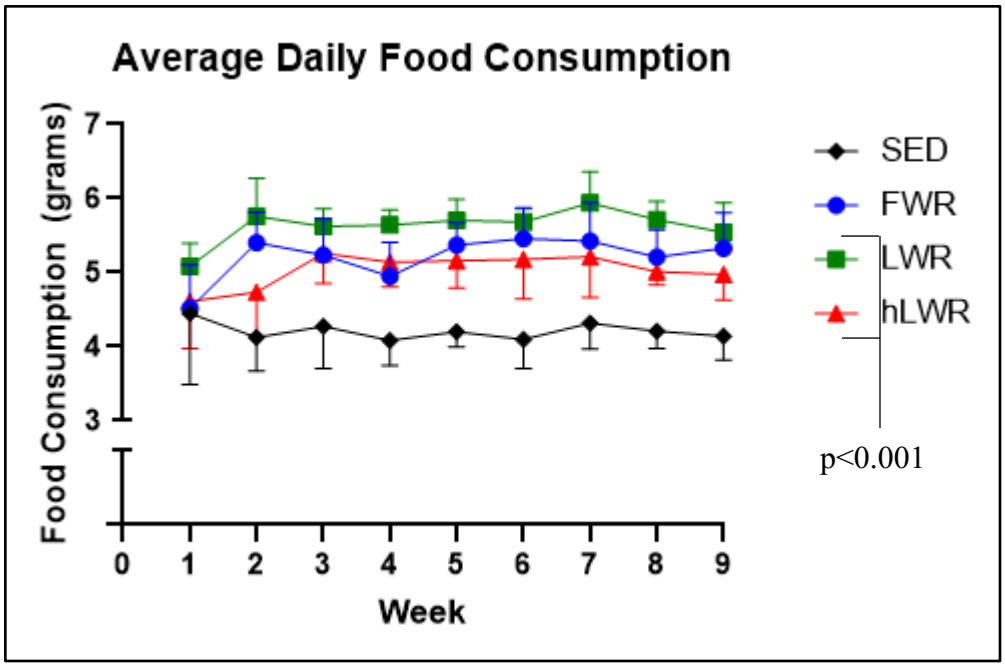

Figure 8. Average daily food consumption over the 9-week protocol. Food consumption was recorded on a daily basis for all mice throughout the 9-week protocol. There was a main effect of treatment as mice in the free wheel running (FWR), loaded wheel running (LWR), and high loaded wheel running (HLWR) groups all consumed more food than the sedentary (SED) group, while there was no effect of time on food consumption. Data are expressed as mean ± SD.

Running Characteristics

After the acclimation week (week 1), there were no treatment x time interactions in running distance or duration ($F=1.215$, $p=0.327$; $F=0.542$, $p=0.715$, respectively). There was also no main effect of time in running distance or duration ($F=0.967$, $p=0.407$; $F=1.517$ $p=0.239$, respectively). Running distance and duration appears to peak in week five or six and was maintained for the remainder of the training protocol, especially in the FWR and LWR groups (Figures 9 and 10, respectively). Running velocity revealed no treatment x time

interaction (F=2.104, p=0.110); however, there was a main effect of time (Figure 11, F=3.482, p=0.046), where running distance appeared to increase for all treatment groups for a majority of the training protocol.

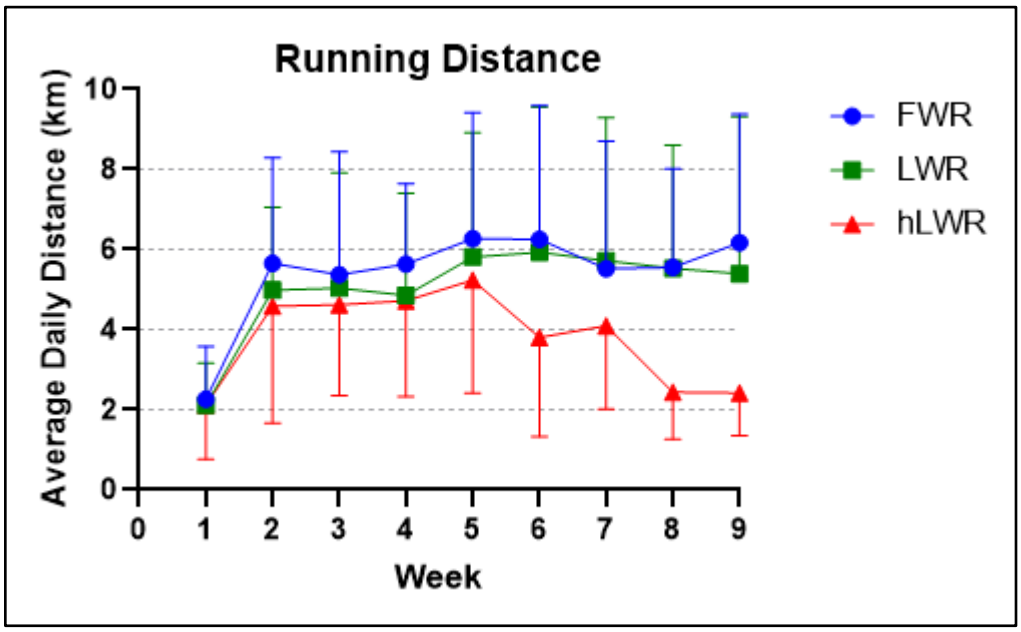

Figure 9. Daily running distance over the 9-week protocol. Running distance was measured manually on a daily basis at a consistent time internal. There was no effect of treatment or time. Free wheel running (FWR). Loaded wheel running (LWR). High loaded wheel running (HLWR). Data are expressed as mean ± SD.

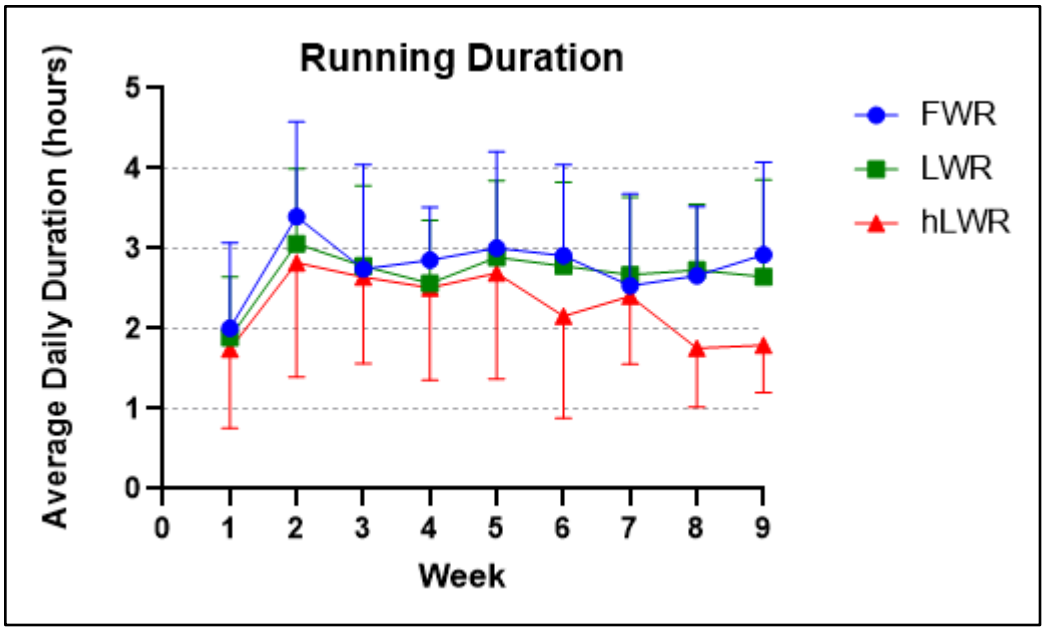

Figure 10. Daily running duration over the 9-week protocol. Running duration was measured manually on a daily basis at a consistent time internal. There was no effect of treatment or time. Free wheel running (FWR). Loaded wheel running (LWR). High loaded wheel running (HLWR). Data are expressed as mean ± SD.

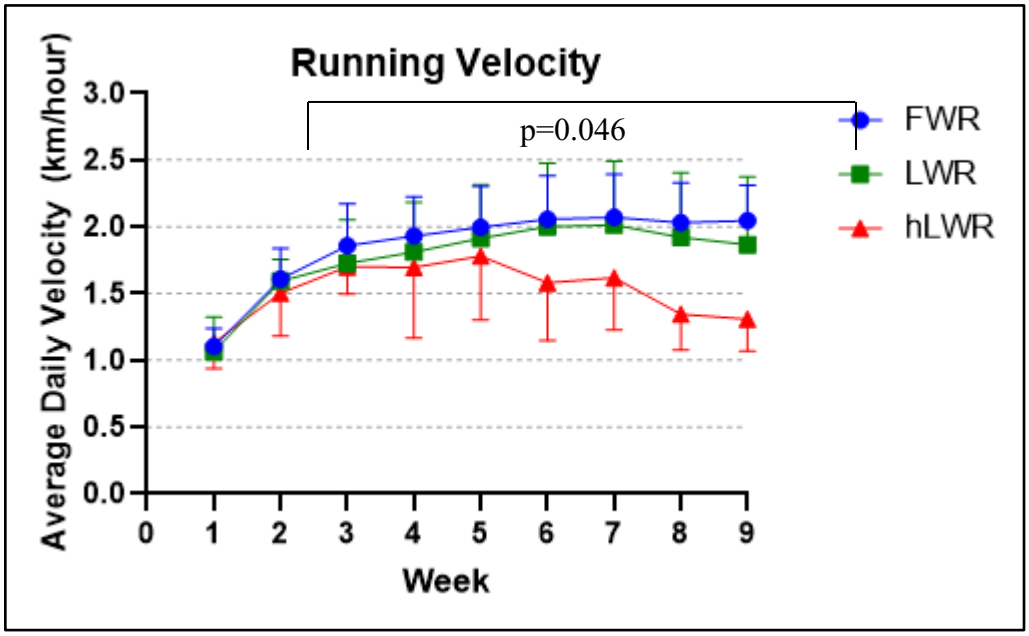

Figure 11. Daily running velocity over the 9-week protocol. Running velocity is a function of daily average distance divided by running duration. There was a main effect of time but not treatment. Free wheel running (FWR). Loaded wheel running (LWR). High loaded wheel running (HLWR). Data are expressed as mean ± SD.

Isometric Forelimb Grip Strength Test

There was no treatment x time effect in grip strength (F=0.743, p=0.819); however, there was a main effect of time where grip strength decreased (F= 12.271, p<0.0001) during the training protocol (Figure 12).

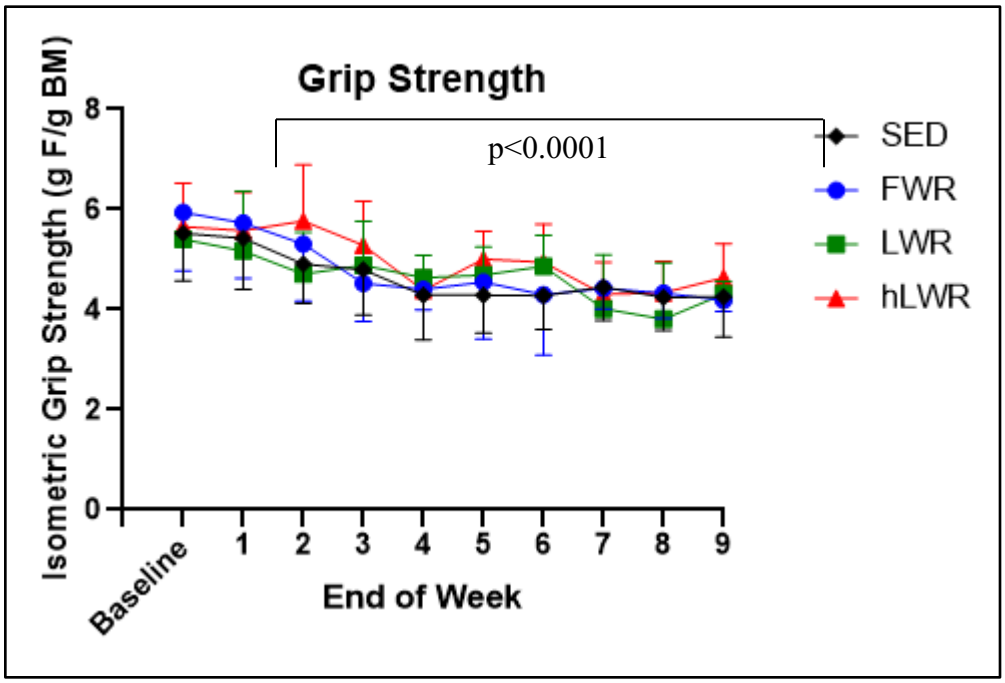

Figure 12. In vivo isometric grip strength throughout training protocol. Grip strength was recorded on a weekly basis over the 9-week protocol. There was a main effect of time, where grip strength decreased but not treatment. Free wheel running (FWR). Loaded wheel running (LWR). High loaded wheel running (HLWR). Data are expressed as mean ± SD.

In Situ Contractile Function

There were no significant differences in twitch or normalized peak force (N/g GPS) between groups (Table 3). Figure 13 depicts the force-frequency curve with all 11 ascending contractions.

Table 3: *In Situ* Contractile Function Test						
	SED	FWR	LWR	HLWR	P-value F-value	Effect Size
Twitch Force (N/g GPS)	2.96±0.47	3.16±0.60	3.19±0.58	3.42±0.77	P=0.422 F=.972	0.108
Peak Force (N/g GPS)	11.42±1.77	11.36±2.64	13.04±2.87	13.12±1.70	P=0.236 F=1.516	0.159

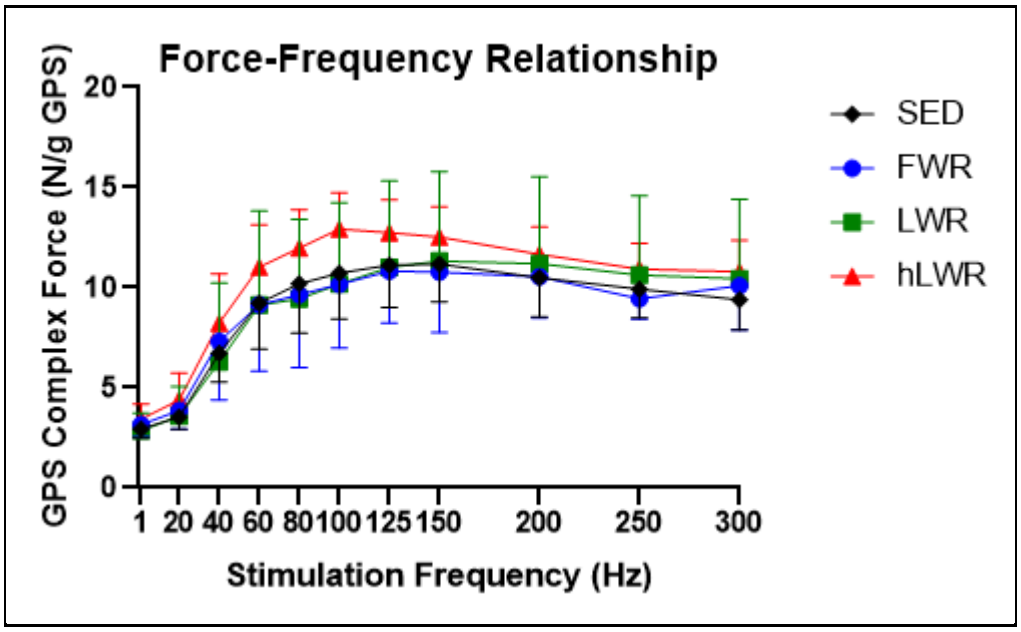

Figure 13. In situ force-frequency curve. Force of the GPS complex normalized to GPS tissue mass with 11 ascending contractions. Free wheel running (FWR). Loaded wheel running (LWR). High loaded wheel running (HLWR). Data are expressed as mean ± SD.

Tissue Mass

SOL mass was 20.4% and 18.8% greater in the HLWR ($p<0.001$) and FWR ($p=0.009$) groups, compared to the SED group, respectively. No differences were observed in Heart, GAS, PLT, or TRI tissue mass (Table 4).

Table 4: Tissue Mass (mg tissue/g body mass)

	SED	FWR	LWR	HLWR	P-value	Effect Size
Heart	4.66±0.27	4.76±0.36	4.98±0.57	4.86±0.23	0.334	0.130
GAS	4.70±0.20	4.56±0.35	4.56±0.16	4.78±0.39	0.498	0.093
PLT	0.61±0.06	0.64±0.03	0.64±0.03	0.63±0.06	0.671	0.061
SOL	0.28±0.03	0.33±0.04*	0.31±0.02	0.34±0.03*	0.004	0.423
TRI	4.00±0.30	3.77±0.45	3.90±0.39	4.14±0.30	0.328	0.131

* Indicates significantly different than SED

Cross-Sectional Area and Minimum Feret Diameter

There were no statistically significant differences in fCSA between treatment groups; however, minimum feret diameter for the PLT was significantly greater in the HLWR group, compared to the SED group (Table 5). Further, there does not appear to be any proportional shifts in fCSA in the GAS, PLT, SOL, and TRI (Figures 14-17, respectively), although statistical analyses were not performed for these assessments.

Table 5.1: Fiber Cross-Sectional Area (μm²)					
	SED	FWR	LWR	HLWR	P-value
GAS	2434±263	2443±313	2410±143	2451±282	0.996
PLT	2164±193	2514±261	2380±514	2646±404	0.082
SOL	1713±331	1973±169	1963±357	1747±167	0.27
TRI	2506±338	2003±70	2473±335	2674±280	0.097
Table 5.2: Minimum Feret Diameter (μm)					
	SED	FWR	LWR	HLWR	P-Value
GAS	46.6±3.07	46.9±2.83	46.2±2.40	46.84±2.56	0.986
PLT	43.1±2.52	47.0±1.56	45.4±4.13	48.2±4.20*	0.048
SOL	39.7±3.84	44.4±3.21	42.4±4.42	39.8±1.72	0.103
TRI	46.7±3.46	42.43±1.24	46.4±3.21	48.0±2.60	0.201
* Indicates significantly different than SED					

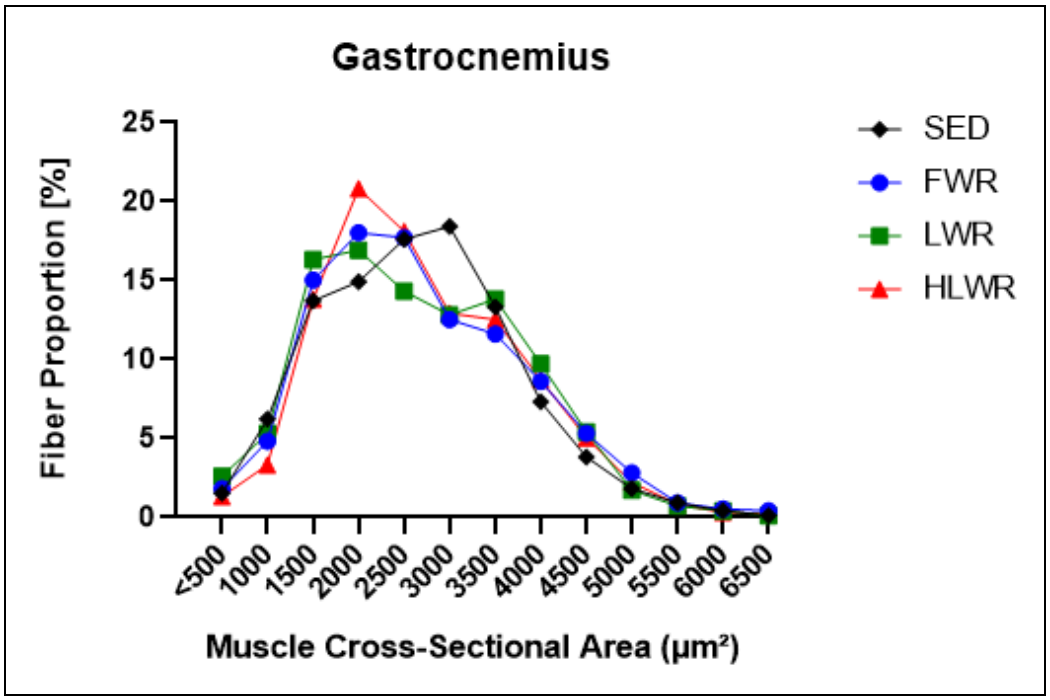

Figure 14. Distribution of fiber cross-sectional area in the gastrocnemius muscle

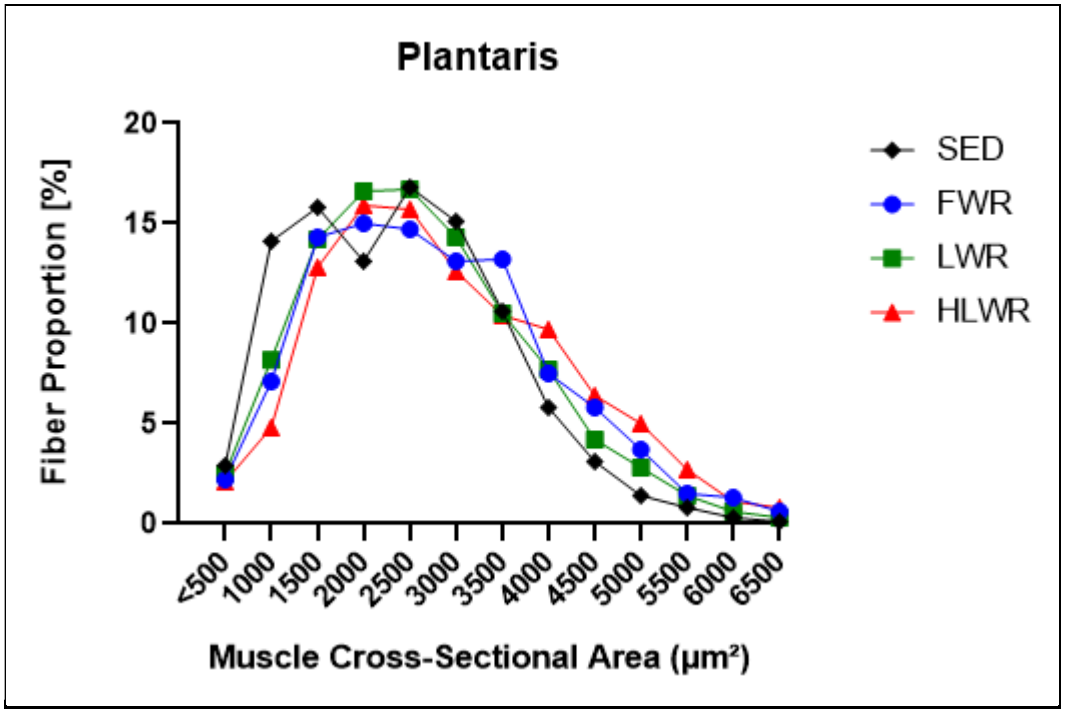

Figure 15. Distribution of fiber cross-sectional area in the plantaris muscle

Figure 16. Distribution of fiber cross-sectional area in the soleus muscle

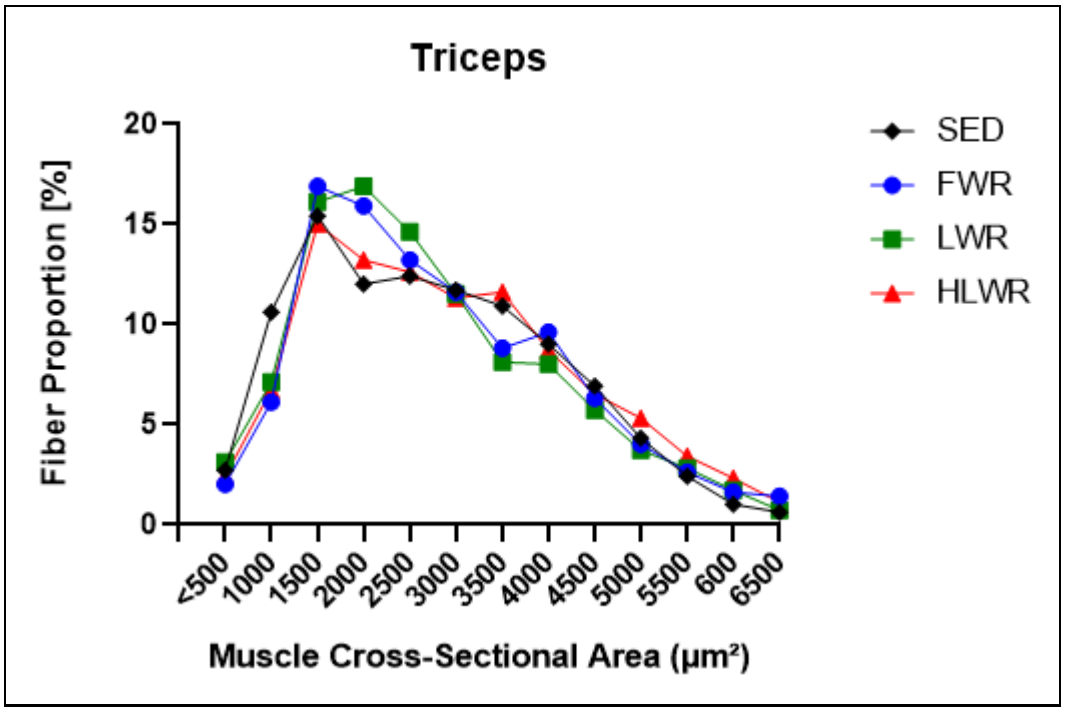

Figure 17. Distribution of fiber cross-sectional area in the triceps brachii muscle

Chapter 5. Discussion

Existing resistance exercise models in rodents have proven invaluable for skeletal muscle research; however, many of these models are invasive, involuntary, and/or time and labor intensive. Loaded wheel running in general is an excellent model that not only induces similar muscular adaptations as those observed in other well-accepted resistance exercise training models, but also provides a chronic, low-stress exercise stimulus for the animal with minimal time/labor commitment by the researcher. Additionally, the LWR model requires minimal direct intervention from the researcher, thus entire cohorts of mice can easily be exercise trained simultaneously for short- or long-term intervention studies. Further, unlike the synergist ablation model, muscular adaptations are reversible as the training stimulus (the running wheel) can simply be removed. However, with the friction-based method of wheel load application, comparatively low wheel load fails to deter mice from running great distances (i.e., too little resistance), or on the contrary with moderate to high added wheel load, the mice discontinue running nearly entirely due to the initial resistance being too great to initiate the wheel to spin (i.e., too much load). The progressive weighted-wheel-running (PoWeR) LWR model developed by Dungan et al. (2019) yields significant muscular adaptations, such as fiber hypertrophy, but also promotes a shift to a more oxidative phenotype. A primary limitation of PoWeR as a "resistance-based" model is that it elicits a higher-volume (distance) and lower-load (resistance) stimulus, more reflective of a concurrent training regimen providing a combination of both resistance and endurance stimuli. Therefore, the purpose of this study was to develop a novel high-loaded wheel running (HLWR) model for mice that modifies the PoWeR model to provide more of a

resistance-biased stimulus where external load is applied and progressively increased, enabling mice to continue running but at much higher loads than previously used.

Logistical Considerations of the HLWR Experimental Model

While the present study fails to display any statistically significant decrease in running distance in the HLWR group, the significance of this novel HLWR model is that it demonstrates mice can continue to run with relatively high loads applied to the wheel. The highest loads of 10-12.5 g in the HLWR model (equivalent to ~40-50% of the mouse's body mass) are considerably higher than those of the PoWeR model (maximum = 6 g), or approximately twice the wheel resistance. Although not statistically significant, there appears to be a stark decline in running distance as wheel load progressed past 7.5 g in week 6 and beyond of the HLWR model. The failure of high wheel loads in our HLWR model to significantly attenuate running distance is a limitation to these findings; however, this may be mitigated with larger sample sizes as there is very high variability in running performance within the groups. Additionally, the LWR group maintained running distance over the 9-week protocol and was similar to the FWR running distances, which is consistent with the data in the originally published PoWeR study (Dungan et al., 2019).

Although it can be difficult to assess a mouse's inclination to consistently run within the first week of acclimation to wheel running, it is unlikely a mouse will drastically change its behavior over a 9-week intervention period. While C57BL/6J mice are generally very good runners compared to other inbred strains, running 3.8-8.4km/day (Lightfoot et al., 2004, 2010), some mice will just not run enough to provide a substantial stimulus to induce muscular adaptations. Thus, it is recommended to implement a minimum threshold cut-off for continued inclusion of any particular mouse in wheel running groups. The minimum

threshold cut-off that was used for this study was an average running distance of <2 km/day during the second and third weeks of training. In this case, if any particular mouse does not meet the minimum threshold of 2 km/day, the wheel should be locked, and the mouse should be reassigned to the sedentary group for the remainder of the 9-week intervention.

Implementing this minimum threshold cut-off will decrease variability in running statistics and ensure that mice will acquire an adequate training stimulus over the 9-week protocol. This is in the spirit of the three "R's" of animal research, specifically reduction. Furthermore, it is important to have a built-in contingency plan if a mouse fails to run a certain distance when high wheel loads are applied. It is suggested that if any particular mouse does not run at least 0.25 km within a 24-hour period after adding load, it may be necessary to reduce the load back to the previous load to ensure that the mouse will continue training for the remainder of the 9-week protocol. It would be unfortunate to have a mouse successfully run for the majority of the protocol only to be removed from the study because it could not reach the next stage at very high wheel loads. Reducing load slightly to ensure continued running maximizes usage of an individual animal without compromising welfare. During this study, the contingency plan had to be implemented for three of the seven mice in the HLWR group, whereby load needed to be reduced to 10 g or 7.5 g at one point during the 9-week training protocol but was never implemented in the LWR group. Lastly, it is also important to track daily (or at least weekly) food consumption to ensure that mice are consuming enough food to compensate for the increased physical activity, there was a significant increase in food intake in the running wheel groups, compared to the SED group. This is relatively simple when mice are individually housed. Expect ~20% greater food intake compared to sedentary mice (Manzanares et al., 2019).

Comparison to Other Loaded Wheel Models

It is difficult to directly compare my results (e.g., running distances) to those previously published models, especially the friction-based loaded wheel models. The loaded wheel running model described by Konhilas et al. (2005) compared both low resistance (LR) and high resistance (HR) groups, where the LR group had load progressively increased up to 5 grams over seven weeks, and running distance was maintained at 4-5 km/day, whereas the HR group peaked at 5 km/day in week two, but steadily declined towards <1 km/day as load was progressively increased to 12 grams (Konhilas et al., 2005). The loaded wheel running model reported by Soffe et al., (2016) also had a LR and HR group, where the LR group had load progressively increased up to 4 grams over 10 weeks, and running distance peaked at almost 10 km/day in week two and steadily declined to 1.61 km/day in the final week. Similarly, the HR group peaked at almost 10 km/day in week two, but steadily declined towards <1 km/day as load was progressively increased to six grams (Soffe et al., 2016). Thus, a gram of added load via friction may not add the same perceived resistance (by the mouse) as a gram of added load via asymmetrical loading, such as the PoWeR model, or even other friction-based models. As a direct comparison to the originally published data of the PoWeR model, Dungan et al. (2019) reported running distances of ~10-12 km per day, whereas my mice performing a similar loading regimen as the PoWeR LWR protocol ran only ~5-6 km per day. This large discrepancy could be attributed to the fact that this present study used male mice, compared to the female C57BL/6 mice used by Dungan et al. (2019). It has been reported that female mice run ~20-40% farther than male mice (Bartling et al., 2017; Lightfoot et al., 2004). Furthermore, Dungan et al. (2019) used wheels with a metal rod running surface, which may lead to better running performance compared to our solid-

surface plastic wheels. Our laboratory also reported previously that young female C57BL/6 mice ran on average 8-10 km/day on the same solid-surface plastic running wheel setup (Zwetsloot et al., 2008). Therefore, in other unique laboratory settings, pilot testing is strongly recommended to determine running performance of mice due to factors such as strain, sex, wheel type, and individual variation.

Measures of Muscle Strength and Hypertrophy

Unexpectedly, there was an overall decline in grip strength in all mice over the 9-week intervention period, compared to the baseline measurement ($p=0.003$); however, there were no significant differences observed in grip strength between groups. This decline can in large part be attributed to the frequent handling of mice. It is possible that with the mice being handled multiple times a week, it may be likely they were not as distressed when the grip strength test was performed, and thus they grasped onto the bar less strongly over time. There may also have been a learning response to the grip strength test, independent of the lower stress due to frequent handling, whereby repeating the test numerous times caused the mice learned there was no imminent danger, thus not grasping onto the bar as hard as possible. Additionally, unlike the wire bar running wheels, my running wheels had a smooth plastic surface which might not be the most conducive surface type for mice to grasp onto with their forepaws and subsequently elicit a forearm/grip strength response.

Isometric strength of the gastrocnemius, plantaris, soleus (GPS) complex was measured using an *in situ* muscle function test via a force-frequency curve. Both isometric twitch force and peak force were derived from those data, where peak force was mostly observed between 100-200 Hz stimulation frequencies. To my knowledge, this is the first loaded wheel running study to report muscle strength outcomes after the intervention period.

Unfortunately, this study failed to observe significant increases in GPS complex strength in response to wheel running; however, as seen in the force-frequency curve (Figure 13), force measurements often declined as stimulation frequency increased beyond 150 to 200 Hz. One possible explanation is retrograde stimulation of the sciatic nerve, where less net amperage reaches the desired muscle group, causing a weaker contraction. It is also possible that the muscle contraction is so strong at high stimulation frequencies that it causes slippage of the suture that attaches the Achilles tendon to the servomotor, attenuating force transmitted to the servomotor, thus differences in strength that may have existed between groups were not able to be observed. Additionally, the GAS, which comprises approximately 85% of the mass of the GPS complex, did not display an increase in muscle mass or fiber size, whereas the SOL and PLT displayed ~20% and 12% increase, respectively. Thus, any adaptations to isometric strength in the SOL and PLT could have been masked by the relatively large GAS muscle. As improvements to muscular strength are a hallmark adaptation to resistance exercise, more data assessing strength adaptations to individual hindlimb muscles involved in loaded wheel running would be beneficial to confirm whether or not the HLWR model is more reflective of resistance exercise, compared to other LWR models such as PoWeR (Dungan et al., 2019).

The SOL muscle of FWR and HLWR mice displayed a 18.8% and 20.4% increase in muscle mass, respectively. The magnitude of SOL mass growth is similar to previous literature employing loaded wheel running (Dungan et al., 2019; Konhilas et al., 2005; Legerlotz et al., 2008; Soffe et al., 2016). Those same studies also displayed a 15-30% increase in mass of other plantar flexor muscles, such as the GAS and PLT, whereas I observed no increase in the mass of other muscles in response to the novel HLWR model,

which is another limitation to this study. Of note, the FWR group displayed nearly the same SOL muscle growth as the HLWR, whereas the LWR group did not show any growth. This could be more evidence that there is insufficient data to assess muscular adaptations to the respective training protocols and more samples may be needed to increase the statistical power of this study. There was also no statistically significant increase in fCSA of any muscles analyzed after the 9-week training period, though the PLT and TRI are trending towards larger fibers in the HLWR group ($p=0.082$ and $p=0.097$, respectively). Minimum feret diameter, which is a measure of fiber size with reduced influence of longitudinal fibers, was also measured. I observed that PLT was significantly greater in the HLWR group, compared to the SED group ($p=0.048$). Interestingly, there was no concomitant increase in SOL fCSA with tissue mass. There was also no discernable change to distribution of fCSA, so it cannot be speculated whether there was a shift toward more slow-twitch oxidative or fast-twitch glycolytic fibers, as slower-twitch fibers tend to be smaller and faster-twitch fibers tend to be larger. The LWR group, which utilized an identical training protocol to the PoWeR model, failed to replicate the results shown by its developers, including a 15-30% increase in both PLT and SOL muscle mass and fCSA, as well as a shift in fiber-type from glycolytic to more oxidative within those muscles (Dungan et al., 2019). This could be because with lower loads, the mice must run much greater distances (i.e., 10-12 km/day performed in the initial PoWeR model) to perform comparable training volume as the HLWR group. Combined, these data suggest that muscle hypertrophy in response to our novel HLWR resistance training model may be limited to muscle that are of a more slow-twitch or oxidative phenotype; however, further investigation is needed to confirm this notion, as the data are underpowered to determine any significant differences at this time.

Practical Aspects of the Loaded Wheel Running Model

Last, as with other wheel running models, this model helps fulfill another one of the three "R's" of animal research - refinement. As wheel running is entirely voluntary, this model is non-invasive and tremendously less stressful for mice compared to other hypertrophy models, specifically synergist ablation, or other models that require days or weeks of operant conditioning. Additionally, this model is of extremely low cost to employ, which may be enticing to other laboratories that do not have the large budget to purchase rodent running wheel wheel cages and software from scientific vendors, which can cost many thousands of dollars to train an entire cohort of mice.

In conclusion, the practical application of this novel progressive high-load wheel running model is a simple, inexpensive, high-throughput, and low stress resistance exercise intervention for mice. This study is not without limitations; namely the HLWR group failed to show a statistically significant decrease in running distance compared to the LWR or FWR group. Thus, it cannot be said that this model is more resistance-exercise biased than previously existing models, such as PoWeR. That said, this study demonstrates the feasibility of HLWR since mice are clearly capable of running with almost twice the added load as that used in the PoWeR model. I also observed very limited muscle growth, no fiber hypertrophy, nor improvements in muscular strength in response to 9 weeks of loaded wheel running. Last, in many aspects, I believe that the data are underpowered. The sample size of mice in wheel running groups included for analyses was far less than desired and previous literature discussing voluntary wheel running, thus more data are needed to assess the effectiveness of this model. This is in part due to higher than anticipated attrition of mice that were initially placed into the wheel running groups. Consequently, the sedentary group is overpowered

(n=13), while running wheel groups are underpowered (average n=5 per group). Subsequent power analyses based on running statistics and tissue masses indicate that 8-9 mice are needed per wheel running group, while there is only an average of 5 per group. Future directions for this project to correct this discrepancy is to train an additional fifteen mice split between the three wheel running groups to collect additional data.

References

Aagaard, P., Andersen, J. L., Dyhre-Poulsen, P., Leffers, A.-M., Wagner, A., Magnusson, S. P., Halkjaer-Kristensen, J., & Simonsen, E. B. (2001). A mechanism for increased contractile strength of human pennate muscle in response to strength training: Changes in muscle architecture. *The Journal of Physiology*, *534*(2), 613–623. https://doi.org/10.1111/j.1469-7793.2001.t01-1-00613.x

Allen, D. L., Harrison, B. C., Maass, A., Bell, M. L., Byrnes, W. C., & Leinwand, L. A. (2001). Cardiac and skeletal muscle adaptations to voluntary wheel running in the mouse. *Journal of Applied Physiology*, *90*(5), 1900–1908. https://doi.org/10.1152/jappl.2001.90.5.1900

Andersen, J. L., & Aagaard, P. (2000). Myosin heavy chain IIX overshoot in human skeletal muscle. *Muscle & Nerve*, *23*(7), 1095–1104. https://doi.org/10.1002/1097-4598(200007)23:7<1095::aid-mus13>3.0.co;2-o

Baar, K., & Esser, K. (1999). Phosphorylation of $p70^{S6k}$ correlates with increased skeletal muscle mass following resistance exercise. *American Journal of Physiology-Cell Physiology*, *276*(1), C120–C127. https://doi.org/10.1152/ajpcell.1999.276.1.C120

Baldwin, K. M., Valdez, V., Herrick, R. E., MacIntosh, A. M., & Roy, R. R. (1982). Biochemical properties of overloaded fast-twitch skeletal muscle. *Journal of Applied Physiology*, *52*(2), 467–472. https://doi.org/10.1152/jappl.1982.52.2.467

Bamman, M. M., Petrella, J. K., Kim, J., Mayhew, D. L., & Cross, J. M. (2007). Cluster analysis tests the importance of myogenic gene expression during myofiber hypertrophy in humans. *Journal of Applied Physiology*, *102*(6), 2232–2239. https://doi.org/10.1152/japplphysiol.00024.2007

Bellamy, L. M., Joanisse, S., Grubb, A., Mitchell, C. J., McKay, B. R., Phillips, S. M., Baker, S., & Parise, G. (2014). The Acute Satellite Cell Response and Skeletal Muscle Hypertrophy following Resistance Training. *PLoS ONE*, *9*(10), e109739. https://doi.org/10.1371/journal.pone.0109739

Bloemberg, D., & Quadrilatero, J. (2012). Rapid Determination of Myosin Heavy Chain Expression in Rat, Mouse, and Human Skeletal Muscle Using Multicolor Immunofluorescence Analysis. *PLoS ONE*, *7*(4), e35273. https://doi.org/10.1371/journal.pone.0035273

Bodine, S. C. (2001). Identification of Ubiquitin Ligases Required for Skeletal Muscle Atrophy. *Science*, *294*(5547), 1704–1708. https://doi.org/10.1126/science.1065874

Brodal, P., Ingjer, F., & Hermansen, L. (1977). Capillary supply of skeletal muscle fibers in untrained and endurance-trained men. *American Journal of Physiology-Heart and Circulatory Physiology*, *232*(6), H705–H712. https://doi.org/10.1152/ajpheart.1977.232.6.H705

Call, J. A., Donet, J., Martin, K. S., Sharma, A. K., Chen, X., Zhang, J., Cai, J., Galarreta, C. A., Okutsu, M., Du, Z., Lira, V. A., Zhang, M., Mehrad, B., Annex, B. H., Klibanov, A. L., Bowler, R. P., Laubach, V. E., Peirce, S. M., & Yan, Z. (2017). Muscle-derived extracellular superoxide dismutase inhibits endothelial activation and protects against multiple organ dysfunction syndrome in mice. *Free Radical Biology and Medicine*, *113*, 212–223. https://doi.org/10.1016/j.freeradbiomed.2017.09.029

Call, J. A., Mckeehen, J. N., Novotny, S. A., & Lowe, D. A. (2010). Progressive resistance voluntary wheel running in the mdx mouse. *Muscle & Nerve*, *42*(6), 871–880. https://doi.org/10.1002/mus.21764

Castro, B., & Kuang, S. (2017). Evaluation of Muscle Performance in Mice by Treadmill Exhaustion Test and Whole-limb Grip Strength Assay. BIO-PROTOCOL, 7(8). https://doi.org/10.21769/BioProtoc.2237

Cheek, D. B. (1985). The control of cell mass and replication. The DNA unit—A personal 20-year study. *Early Human Development*, *12*(3), 211–239. https://doi.org/10.1016/0378-3782(85)90144-6

Chi, M. M., Hintz, C. S., Coyle, E. F., Martin, W. H., Ivy, J. L., Nemeth, P. M., Holloszy, J. O., & Lowry, O. H. (1983). Effects of detraining on enzymes of energy metabolism in individual human muscle fibers. *American Journal of Physiology-Cell Physiology*, *244*(3), C276–C287. https://doi.org/10.1152/ajpcell.1983.244.3.C276

Choi, S. J. (2014). Differential susceptibility on myosin heavy chain isoform following eccentric-induced muscle damage. *Journal of Exercise Rehabilitation*, *10*(6), 344–348. https://doi.org/10.12965/jer.140171

Cholewa, J., Guimarães-Ferreira, L., da Silva Teixeira, T., Naimo, M. A., Zhi, X., de Sá, R. B. D. P., Lodetti, A., Cardozo, M. Q., & Zanchi, N. E. (2014). Basic models modeling resistance training: an update for basic scientists interested in study skeletal muscle hypertrophy: Basic models modeling resistance training. *Journal of Cellular Physiology*, *229*(9), 1148–1156. https://doi.org/10.1002/jcp.24542

Cork, G. K., Thompson, J., & Slawson, C. (2018). Real Talk: The Inter-play Between the mTOR, AMPK, and hexosamine biosynthetic pathways in cell signaling. *Frontiers in Endocrinology*, *9*, 522. https://doi.org/10.3389/fendo.2018.00522

Cui, D., Drake, J. C., Wilson, R. J., Shute, R. J., Lewellen, B., Zhang, M., Zhao, H., Sabik, O. L., Onengut, S., Berr, S. S., Rich, S. S., Farber, C. R., & Yan, Z. (2020). A novel

voluntary weightlifting model in mice promotes muscle adaptation and insulin sensitivity with simultaneous enhancement of autophagy and mTOR pathway. *The FASEB Journal*, *34*(6), 7330–7344. https://doi.org/10.1096/fj.201903055R

Cuthbertson, D. J., Babraj, J., Smith, K., Wilkes, E., Fedele, M. J., Esser, K., & Rennie, M. (2006). Anabolic signaling and protein synthesis in human skeletal muscle after dynamic shortening or lengthening exercise. *American Journal of Physiology-Endocrinology and Metabolism*, *290*(4), E731–E738. https://doi.org/10.1152/ajpendo.00415.2005

De Bono, J. P., Adlam, D., Paterson, D. J., & Channon, K. M. (2006). Novel quantitative phenotypes of exercise training in mouse models. *American Journal of Physiology-Regulatory, Integrative and Comparative Physiology*, *290*(4), R926–R934. https://doi.org/10.1152/ajpregu.00694.2005

DeFronzo, R. A., & Tripathy, D. (2009). Skeletal muscle insulin resistance is the primary defect in type 2 diabetes. *Diabetes Care*, *32*(suppl_2), S157–S163. https://doi.org/10.2337/dc09-S302

D'Hulst, G., Palmer, A. S., Masschelein, E., Bar-Nur, O., & De Bock, K. (2019). Voluntary resistance running as a model to induce mtor activation in mouse skeletal muscle. *Frontiers in Physiology*, *10*, 1271. https://doi.org/10.3389/fphys.2019.01271

Duncan, N. d., Williams, D. a., & Lynch, G. s. (1998). Adaptations in rat skeletal muscle following long-term resistance exercise training. *European Journal of Applied Physiology & Occupational Physiology*, *77*(4), 372–278.

Dungan, C. M., Murach, K. A., Frick, K. K., Jones, S. R., Crow, S. E., Englund, D. A., Vechetti, I. J., Figueiredo, V. C., Levitan, B. M., Satin, J., McCarthy, J. J., &

Peterson, C. A. (2019). Elevated myonuclear density during skeletal muscle hypertrophy in response to training is reversed during detraining. *American Journal of Physiology-Cell Physiology*, *316*(5), C649–C654. https://doi.org/10.1152/ajpcell.00050.2019

Folland, J. P., & Williams, A. G. (2007). The adaptations to strength training: morphological and neurological contributions to increased strength. *Sports Medicine*, *37*(2), 145–168. https://doi.org/10.2165/00007256-200737020-00004

Frontera, W. R., & Ochala, J. (2015). Skeletal muscle: a brief review of structure and function. *Calcified Tissue International*, *96*(3), 183–195. https://doi.org/10.1007/s00223-014-9915-y

Frost, H. M. (1997). On our age-related bone loss: insights from a new paradigm. *Journal of Bone and Mineral Research*, *12*(10), 1539–1546. https://doi.org/10.1359/jbmr.1997.12.10.1539

Fry, C. S., Lee, J. D., Jackson, J. R., Kirby, T. J., Stasko, S. A., Liu, H., Dupont-Versteegden, E. E., McCarthy, J. J., & Peterson, C. A. (2014). Regulation of the muscle fiber micro environment by activated satellite cells during hypertrophy. *The FASEB Journal*, *28*(4), 1654–1665. https://doi.org/10.1096/fj.13-239426

Gavin, T. P. (2009). Basal and exercise-induced regulation of skeletal muscle capillarization: *Exercise and Sport Sciences Reviews*, *37*(2), 86–92. https://doi.org/10.1097/JES.0b013e31819c2e9b

Gavin, T. P., Spector, D. A., Wagner, H., Breen, E. C., & Wagner, P. D. (2000). Nitric oxide synthase inhibition attenuates the skeletal muscle VEGF mRNA response to exercise.

Journal of Applied Physiology, *88*(4), 1192–1198. https://doi.org/10.1152/jappl.2000.88.4.1192

Goh, J., & Ladiges, W. (2015). Voluntary wheel running in mice. *Current Protocols in Mouse Biology*, *5*(4), 283–290. https://doi.org/10.1002/9780470942390.mo140295

Godwin, J. S., Hodgman, C. F., Needle, A. R., Zwetsloot, K. A., & Andrew, R. (2020). Whole-body heat shock accelerates recovery from impact- induced skeletal muscle damage in mice. *Conditioning Medicine* 2020. 2(4): 184-191.

Goldberg, A. L. (1968). Protein synthesis during work-induced growth of skeletal muscle. *The Journal of Cell Biology*, *36*(3), 653–658. https://doi.org/10.1083/jcb.36.3.653

Gwinn, D. M., Shackelford, D. B., Egan, D. F., Mihaylova, M. M., Mery, A., Vasquez, D. S., Turk, B. E., & Shaw, R. J. (2008). AMPK phosphorylation of raptor mediates a metabolic checkpoint. *Molecular Cell*, *30*(2), 214–226. https://doi.org/10.1016/j.molcel.2008.03.003

Hakkinen, K., Newton, R. U., Gordon, S. E., McCormick, M., Volek, J. S., Nindl, B. C., Gotshalk, L. A., Campbell, W. W., Evans, W. J., Hakkinen, A., Humphries, B. J., & Kraemer, W. J. (1998). Changes in muscle morphology, electromyographic activity, and force production characteristics during progressive strength training in young and older men. *The Journals of Gerontology Series A: Biological Sciences and Medical Sciences*, *53A*(6), B415–B423. https://doi.org/10.1093/gerona/53A.6.B415

Handschin, C., Rhee, J., Lin, J., Tarr, P. T., & Spiegelman, B. M. (2003). An autoregulatory loop controls peroxisome proliferator-activated receptor coactivator 1 expression in muscle. *Proceedings of the National Academy of Sciences*, *100*(12), 7111–7116. https://doi.org/10.1073/pnas.1232352100

Hardie, D. G. (2003). Minireview: The AMP-activated protein kinase cascade: the key sensor of cellular energy status. *Endocrinology*, *144*(12), 5179–5183. https://doi.org/10.1210/en.2003-0982

Haun, C. T., Vann, C. G., Osburn, S. C., Mumford, P. W., Roberson, P. A., Romero, M. A., Fox, C. D., Johnson, C. A., Parry, H. A., Kavazis, A. N., Moon, J. R., Badisa, V. L. D., Mwashote, B. M., Ibeanusi, V., Young, K. C., & Roberts, M. D. (2019). Muscle fiber hypertrophy in response to 6 weeks of high-volume resistance training in trained young men is largely attributed to sarcoplasmic hypertrophy. *PLOS ONE*, *14*(6), e0215267. https://doi.org/10.1371/journal.pone.0215267

Hawley, J. A. (2009). Molecular responses to strength and endurance training: Are they incompatible? *Applied Physiology, Nutrition, and Metabolism*, *34*(3), 355–361. https://doi.org/10.1139/H09-023

Hikida, R. S., Staron, R. S., Hagerman, F. C., Walsh, S., Kaiser, E., Shell, S., & Hervey, S. (2000). Effects of high-intensity resistance training on untrained older men. ii. muscle fiber characteristics and nucleo-cytoplasmic relationships. *The Journals of Gerontology Series A: Biological Sciences and Medical Sciences*, *55*(7), B347–B354. https://doi.org/10.1093/gerona/55.7.B347

Hill, M., & Goldspink, G. (2003). Expression and splicing of the insulin-like growth factor gene in rodent muscle is associated with muscle satellite (stem) cell activation following local tissue damage. *The Journal of Physiology*, *549*(2), 409–418. https://doi.org/10.1113/jphysiol.2002.035832

Holloszy, J O, & Booth, F. W. (1976). Biochemical adaptations to endurance exercise in muscle. *Annual Review of Physiology*, *38*(1), 273–291. https://doi.org/10.1146/annurev.ph.38.030176.001421

Holloszy, John O. (1967). Biochemical adaptations in muscle effects of exercise on mitochondrial oxygen uptake and respiratory enzyme activity in skeletal muscle. *Journal of Biological Chemistry*, *242*(9), 2278–2282.

Hong, A. R., & Kim, S. W. (2018). Effects of Resistance Exercise on Bone Health. *Endocrinology and Metabolism*, *33*(4), 435. https://doi.org/10.3803/EnM.2018.33.4.435

Hong, S., Chang, Y., Jung, H.-S., Yun, K. E., Shin, H., & Ryu, S. (2017). Relative muscle mass and the risk of incident type 2 diabetes: A cohort study. *PLOS ONE*, *12*(11), e0188650. https://doi.org/10.1371/journal.pone.0188650

Hornberger Jr., T. A., & Farrar, R. P. (2004). Physiological hypertrophy of the fhl muscle following 8 weeks of progressive resistance exercise in the rat. *Canadian Journal of Applied Physiology*, *29*(1), 16–31. https://doi.org/10.1139/h04-002

Huang, H., Regan, K. M., Wang, F., Wang, D., Smith, D. I., van Deursen, J. M. A., & Tindall, D. J. (2005). Skp2 inhibits FOXO1 in tumor suppression through ubiquitin-mediated degradation. *Proceedings of the National Academy of Sciences*, *102*(5), 1649–1654. https://doi.org/10.1073/pnas.0406789102

Huxley, H. E. (1969). The mechanism of muscular contraction. *Science*, *164*(3886), 1356–1366. https://doi.org/10.1126/science.164.3886.1356

Ingalls, C. P., Wenke, J. C., Nofal, T., & Armstrong, R. B. (2004). Adaptation to lengthening contraction-induced injury in mouse muscle. *Journal of Applied Physiology*, *97*(3), 1067–1076. https://doi.org/10.1152/japplphysiol.01058.2003

Ishihara, A., Hirofuji, C., Nakatani, T., Itoh, K., Itoh, M., & Katsuta, S. (2002). Effects of running exercise with increasing loads on tibialis anterior muscle fibres in mice. *Experimental Physiology*, *87*(2), 113–116. https://doi.org/10.1113/eph8702340

Ishihara, A., Roy, R. R., Ohira, Y., Ibata, Y., & Edgerton, V. R. (1998). Hypertrophy of rat plantaris muscle fibers after voluntary running with increasing loads. *Journal of Applied Physiology*, *84*(6), 2183–2189. https://doi.org/10.1152/jappl.1998.84.6.2183

Janssen, I., Heymsfield, S. B., & Ross, R. (2002). Low relative skeletal muscle mass (sarcopenia) in older persons is associated with functional impairment and physical disability. *Journal of the American Geriatrics Society*, *50*(5), 889–896. https://doi.org/10.1046/j.1532-5415.2002.50216.x

Jones, T. W., Walshe, I. H., Hamilton, D. L., Howatson, G., Russell, M., Price, O. J., Gibson, A. S. C., & French, D. N. (2016). Signaling responses after varying sequencing of strength and endurance training in a fed state. *International Journal of Sports Physiology and Performance*, *11*(7), 868–875. https://doi.org/10.1123/ijspp.2015-0534

Kadar, L., Albertsson, M., Areberg, J., Landberg, T., & Mattsson, S. (2006). The prognostic value of body protein in patients with lung cancer. *Annals of the New York Academy of Sciences*, *904*(1), 584–591. https://doi.org/10.1111/j.1749-6632.2000.tb06520.x

Kiens, B., Essen-Gustavsson, B., Christensen, N. J., & Saltin, B. (1993). Skeletal muscle substrate utilization during submaximal exercise in man: Effect of endurance training.

The Journal of Physiology, *469*(1), 459–478. https://doi.org/10.1113/jphysiol.1993.sp019823

Konhilas, J. P., Widegren, U., Allen, D. L., Paul, A. C., Cleary, A., & Leinwand, L. A. (2005). Loaded wheel running and muscle adaptation in the mouse. *American Journal of Physiology-Heart and Circulatory Physiology*, *289*(1), H455–H465. https://doi.org/10.1152/ajpheart.00085.2005

Kraemer, W. J., Deschenes, M. R., & Fleck, S. J. (1988). Physiological adaptations to resistance exercise: implications for athletic conditioning. *Sports Medicine*, *6*(4), 246–256. https://doi.org/10.2165/00007256-198806040-00006

Kurosaka, M., Naito, H., Ogura, Y., Kojima, A., Goto, K., & Katamoto, S. (2009). Effects of voluntary wheel running on satellite cells in the rat plantaris muscle. *Journal of Sports Science & Medicine*, *8*(1), 51–57.

Lambert, M. I., & Noakes, T. D. (1990). Spontaneous running increases VO2max and running performance in rats. *Journal of Applied Physiology*, *68*(1), 400–403. https://doi.org/10.1152/jappl.1990.68.1.400

Larsson, L., Degens, H., Li, M., Salviati, L., Lee, Y. il, Thompson, W., Kirkland, J. L., & Sandri, M. (2019). Sarcopenia: aging-related loss of muscle mass and function. *Physiological Reviews*, *99*(1), 427–511. https://doi.org/10.1152/physrev.00061.2017

Lee, K. R., Cronenwett, J. L., Shlafer, M., Corpron, C., & Zelenock, G. B. (1987). Effect of superoxide dismutase plus catalase on Ca2+ transport in ischemic and reperfused skeletal muscle. *Journal of Surgical Research*, *42*(1), 24–32. https://doi.org/10.1016/0022-4804(87)90060-6

Legerlotz, K., Elliott, B., Guillemin, B., & Smith, H. K. (2008). Voluntary resistance running wheel activity pattern and skeletal muscle growth in rats: Wheel running activity pattern and muscle growth. *Experimental Physiology*, *93*(6), 754–762. https://doi.org/10.1113/expphysiol.2007.041244

Lerman, I., Harrison, B. C., Freeman, K., Hewett, T. E., Allen, D. L., Robbins, J., & Leinwand, L. A. (2002). Genetic variability in forced and voluntary endurance exercise performance in seven inbred mouse strains. *Journal of Applied Physiology*, *92*(6), 2245–2255. https://doi.org/10.1152/japplphysiol.01045.2001

Lessard, S. J., MacDonald, T. L., Pathak, P., Han, M. S., Coffey, V. G., Edge, J., Rivas, D. A., Hirshman, M. F., Davis, R. J., & Goodyear, L. J. (2018). JNK regulates muscle remodeling via myostatin/SMAD inhibition. *Nature Communications*, *9*(1), 3030. https://doi.org/10.1038/s41467-018-05439-3

Lightfoot, J. T., Turner, M. J., Daves, M., Vordermark, A., & Kleeberger, S. R. (2004). Genetic influence on daily wheel running activity level. *Physiological Genomics*, *19*(3), 270–276. https://doi.org/10.1152/physiolgenomics.00125.2004

Lira, V. A., Benton, C. R., Yan, Z., & Bonen, A. (2010). PGC-1α regulation by exercise training and its influences on muscle function and insulin sensitivity. *American Journal of Physiology-Endocrinology and Metabolism*, *299*(2), E145–E161. https://doi.org/10.1152/ajpendo.00755.2009

MacDougall, J. D., Elder, G. C. B., Sale, D. G., Moroz, J. R., & Sutton, J. R. (1980). Effects of strength training and immobilization on human muscle fibres. *European Journal of Applied Physiology and Occupational Physiology*, *43*(1), 25–34. https://doi.org/10.1007/BF00421352

Mackay, A. D., Marchant, E. D., Louw, M., Thomson, D. M., & Hancock, C. R. (2021). Exercise, but not metformin prevents loss of muscle function due to doxorubicin in mice using an in situ method. *International Journal of Molecular Sciences*, *22*(17), 9163. https://doi.org/10.3390/ijms22179163

Manzanares, G., Brito-da-Silva, G., & Gandra, P. G. (2018). Voluntary wheel running: patterns and physiological effects in mice. *Brazilian Journal of Medical and Biological Research*, *52*(1). https://doi.org/10.1590/1414-431x20187830

Masschelein, E., D'Hulst, G., Zvick, J., Hinte, L., Soro-Arnaiz, I., Gorski, T., von Meyenn, F., Bar-Nur, O., & De Bock, K. (2020). Exercise promotes satellite cell contribution to myofibers in a load-dependent manner. *Skeletal Muscle*, *10*(1), 21. https://doi.org/10.1186/s13395-020-00237-2

McGuigan, M. R., Wright, G. A., & Fleck, S. J. (2012). Strength training for athletes: does it really help sports performance? *International Journal of Sports Physiology and Performance*, *7*(1), 2–5. https://doi.org/10.1123/ijspp.7.1.2

Meer, S. F. T. van der, Jaspers, R. T., & Degens, H. (2011). Is the myonuclear domain size fixed? *Journal of Musculoskeletal and Neuronal Interactions*, *11*(4), 286–297.

Meijer, J. H., & Robbers, Y. (2014). Wheel running in the wild. *Proceedings of the Royal Society B: Biological Sciences*, *281*(1786), 20140210. https://doi.org/10.1098/rspb.2014.0210

Miller, M. S., Bedrin, N. G., Ades, P. A., Palmer, B. M., & Toth, M. J. (2015). Molecular determinants of force production in human skeletal muscle fibers: Effects of myosin isoform expression and cross-sectional area. *American Journal of Physiology-Cell Physiology*, *308*(6), C473–C484. https://doi.org/10.1152/ajpcell.00158.2014

Miyazaki, M., & Esser, K. A. (2009). Cellular mechanisms regulating protein synthesis and skeletal muscle hypertrophy in animals. *Journal of Applied Physiology*, *106*(4), 1367–1373. https://doi.org/10.1152/japplphysiol.91355.2008

Mobley, C. B., Holland, A. M., Kephart, W. C., Mumford, P. W., Lowery, R. P., Kavazis, A. N., Wilson, J. M., & Roberts, M. D. (2018). Progressive resistance-loaded voluntary wheel running increases hypertrophy and differentially affects muscle protein synthesis, ribosome biogenesis, and proteolytic markers in rat muscle. *Journal of Animal Physiology and Animal Nutrition*, *102*(1), 317–329. https://doi.org/10.1111/jpn.12691

Mobley, Christopher B., Haun, C. T., Roberson, P. A., Mumford, P. W., Kephart, W. C., Romero, M. A., Osburn, S. C., Vann, C. G., Young, K. C., Beck, D. T., Martin, J. S., Lockwood, C. M., & Roberts, M. D. (2018). Biomarkers associated with low, moderate, and high vastus lateralis muscle hypertrophy following 12 weeks of resistance training. *PLOS ONE*, *13*(4), e0195203. https://doi.org/10.1371/journal.pone.0195203

Murach, K. A., & Bagley, J. R. (2016). Skeletal muscle hypertrophy with concurrent exercise training: contrary evidence for an interference effect. *Sports Medicine*, *46*(8), 1029–1039. https://doi.org/10.1007/s40279-016-0496-y

Murach, K. A., Englund, D. A., Dupont-Versteegden, E. E., McCarthy, J. J., & Peterson, C. A. (2018). Myonuclear domain flexibility challenges rigid assumptions on satellite cell contribution to skeletal muscle fiber hypertrophy. *Frontiers in Physiology*, *9*, 635. https://doi.org/10.3389/fphys.2018.00635

Murach, K. A., McCarthy, J. J., Peterson, C. A., & Dungan, C. M. (2020). Making mice mighty: Recent advances in translational models of load-induced muscle hypertrophy. *Journal of Applied Physiology*, *129*(3), 516–521. https://doi.org/10.1152/japplphysiol.00319.2020

Nakada, S., Ogasawara, R., Kawada, S., Maekawa, T., & Ishii, N. (2016). Correlation between ribosome Biogenesis and the Magnitude of Hypertrophy in Overloaded Skeletal Muscle. *PLOS One*, *11*(1), e0147284. https://doi.org/10.1371/journal.pone.0147284

Pertl, C., Eblenkamp, M., Pertl, A., Pfeifer, S., Wintermantel, E., Lochmüller, H., Walter, M. C., Krause, S., & Thirion, C. (2013). A new web-based method for automated analysis of muscle histology. *BMC Musculoskeletal Disorders*, *14*(1), 26. https://doi.org/10.1186/1471-2474-14-26

Qaisar, R., & Larsson, L. (2014). What determines myonuclear domain size? *Indian Journal of Physiology and Pharmacology*, *58*(1), 1–12.

Reaven, G. M. (2005). The insulin resistance syndrome: definition and dietary approaches to treatment. *Annual Review of Nutrition*, *25*(1), 391–406. https://doi.org/10.1146/annurev.nutr.24.012003.132155

Rodnick, K. J., Reaven, G. M., Haskell, W. L., Sims, C. R., & Mondon, C. E. (1989). Variations in running activity and enzymatic adaptations in voluntary running rats. *Journal of Applied Physiology*, *66*(3), 1250–1257. https://doi.org/10.1152/jappl.1989.66.3.1250

Rosenberger, A., Beijer, Å., Johannes, B., Schoenau, E., Mester, J., Rittweger, J., & Zange, J. (2017). Changes in muscle cross-sectional area, muscle force, and jump performance

during 6 weeks of progressive whole-body vibration combined with progressive, high intensity resistance training. *Journal of Musculoskeletal & Neuronal Interactions*, *17*(2), 38–49.

Rosenblatt, J. D., & Parry, D. J. (1992). Gamma irradiation prevents compensatory hypertrophy of overloaded mouse extensor digitorum longus muscle. *Journal of Applied Physiology*, *73*(6), 2538–2543. https://doi.org/10.1152/jappl.1992.73.6.2538

Rosenblatt, J. David, & Parry, D. J. (1993). Adaptation of rat extensor digitorum longus muscle to gamma irradiation and overload. *Pflügers Archiv European Journal of Physiology*, *423*(3–4), 255–264. https://doi.org/10.1007/BF00374404

Schantz, P. G., & Dhoot, G. K. (1987). Coexistence of slow and fast isoforms of contractile and regulatory proteins in human skeletal muscle fibres induced by endurance raining. *Acta Physiologica Scandinavica*, *131*(1), 147–154. https://doi.org/10.1111/j.1748-1716.1987.tb08216.x

Schantz, P., Henriksson, J., & Jansson, E. (1983). Adaptation of human skeletal muscle to endurance training of long duration. *Clinical Physiology*, *3*(6), 141–151. https://doi.org/10.1111/j.1475-097X.1983.tb00685.x

Schnyder, S., & Handschin, C. (2015). Skeletal muscle as an endocrine organ: PGC-1α, myokines and exercise. *Bone*, *80*, 115–125. https://doi.org/10.1016/j.bone.2015.02.008

Sciarretta, S., Forte, M., Frati, G., & Sadoshima, J. (2018). New insights into the role of mtor signaling in the cardiovascular system. *Circulation Research*, *122*(3), 489–505. https://doi.org/10.1161/CIRCRESAHA.117.311147

Sexton, W. L. (1995). Vascular adaptations in rat hindlimb skeletal muscle after voluntary running-wheel exercise. *Journal of Applied Physiology*, *79*(1), 287–296. https://doi.org/10.1152/jappl.1995.79.1.287

Shanely, R. A., Zwetsloot, K. A., Triplett, N. T., Meaney, M. P., Farris, G. E., & Nieman, D. C. (2014). Human skeletal muscle biopsy procedures using the modified bergström technique. *Journal of Visualized Experiments*, *91*, 51812. https://doi.org/10.3791/51812

Smith, L. R., & Barton, E. R. (2014). SMASH – semi-automatic muscle analysis using segmentation of histology: A MATLAB application. *Skeletal Muscle*, *4*(1), 21. https://doi.org/10.1186/2044-5040-4-21

Snijders, T., Smeets, J. S. J., van Kranenburg, J., Kies, A. K., van Loon, L. J. C., & Verdijk, L. B. (2016). Changes in myonuclear domain size do not precede muscle hypertrophy during prolonged resistance-type exercise training. *Acta Physiologica*, *216*(2), 231–239. https://doi.org/10.1111/apha.12609

Snijders, Tim, Nederveen, J. P., McKay, B. R., Joanisse, S., Verdijk, L. B., van Loon, L. J. C., & Parise, G. (2015). Satellite cells in human skeletal muscle plasticity. *Frontiers in Physiology*, *6*. https://doi.org/10.3389/fphys.2015.00283

Soffe, Z., Radley-Crabb, H. G., McMahon, C., Grounds, M. D., & Shavlakadze, T. (2016). Effects of loaded voluntary wheel exercise on performance and muscle hypertrophy in young and old male C57Bl/6J mice: Exercise and muscle hypertrophy in old mice. *Scandinavian Journal of Medicine & Science in Sports*, *26*(2), 172–188. https://doi.org/10.1111/sms.12416

Szulc, P., Beck, T. J., Marchand, F., & Delmas, P. D. (2004). Low skeletal muscle mass is associated with poor structural parameters of bone and impaired balance in elderly men-the MINOS study. *Journal of Bone and Mineral Research*, *20*(5), 721–729. https://doi.org/10.1359/JBMR.041230

Szulc, P., Munoz, F., Marchand, F., Chapurlat, R., & Delmas, P. D. (2010). Rapid loss of appendicular skeletal muscle mass is associated with higher all-cause mortality in older men: The prospective MINOS study. *The American Journal of Clinical Nutrition*, *91*(5), 1227–1236. https://doi.org/10.3945/ajcn.2009.28256

Tamaki, T., Uchiyama, S., & Nakano, S. (1992). A weight-lifting exercise model for inducing hypertrophy in the hindlimb muscles of rats. *Medicine & Science in Sports & Exercise*, *24*(8), 881–886.

Taylor, N. A. S., & Wilkinson, J. G. (1986). Exercise-induced skeletal muscle growth: hypertrophy or hyperplasia? *Sports Medicine*, *3*(3), 190–200. https://doi.org/10.2165/00007256-198603030-00003

Weber, H., Rauch, A., Adamski, S., Chakravarthy, K., Kulkarni, A., Dogdas, B., Bendtsen, C., Kath, G., Alves, S. E., Wilkinson, H. A., & Chiu, C.-S. (2012). Automated rodent in situ muscle contraction assay and myofiber organization analysis in sarcopenia animal models. *Journal of Applied Physiology*, *112*(12), 2087–2098. https://doi.org/10.1152/japplphysiol.00871.2011

Wen, Y., Murach, K. A., Vechetti, I. J., Fry, C. S., Vickery, C., Peterson, C. A., McCarthy, J. J., & Campbell, K. S. (2018). MyoVision: Software for automated high-content analysis of skeletal muscle immunohistochemistry. *Journal of Applied Physiology*, *124*(1), 40–51. https://doi.org/10.1152/japplphysiol.00762.2017

Weston, A. R., Myburgh, K. H., Lindsay, F. H., Dennis, S. C., Noakes, T. D., & Hawley, J. A. (1996). Skeletal muscle buffering capacity and endurance performance after high-intensity interval training by well-trained cyclists. *European Journal of Applied Physiology*, *75*(1), 7–13. https://doi.org/10.1007/s004210050119

White, Z., Terrill, J., White, R. B., McMahon, C., Sheard, P., Grounds, M. D., & Shavlakadze, T. (2016). Voluntary resistance wheel exercise from mid-life prevents sarcopenia and increases markers of mitochondrial function and autophagy in muscles of old male and female C57BL/6J mice. *Skeletal Muscle*, *6*(1), 45. https://doi.org/10.1186/s13395-016-0117-3

Wilkie, D. R. (1949). The relation between force and velocity in human muscle. *The Journal of Physiology*, *110*(3–4), 249–280. https://doi.org/10.1113/jphysiol.1949.sp004437

Williamson, D. L., Gallagher, P. M., Carroll, C. C., Raue, U., & Trappe, S. W. (2001). Reduction in hybrid single muscle fiber proportions with resistance training in humans. *Journal of Applied Physiology*, *91*(5), 1955–1961. https://doi.org/10.1152/jappl.2001.91.5.1955

Wilson, J. M., Marin, P. J., Rhea, M. R., Wilson, S. M. C., Loenneke, J. P., & Anderson, J. C. (2012). Concurrent training: a meta-analysis examining interference of aerobic and resistance exercises. *Journal of Strength and Conditioning Research*, *26*(8), 2293–2307. https://doi.org/10.1519/JSC.0b013e31823a3e2d

Wirth, O., Gregory, E. W., Cutlip, R. G., & Miller, G. R. (2003). Control and quantitation of voluntary weight-lifting performance of rats. *Journal of Applied Physiology*, *95*(1), 402–412. https://doi.org/10.1152/japplphysiol.00919.2002

Wolfe, R. R. (2006). The underappreciated role of muscle in health and disease. *The American Journal of Clinical Nutrition*, *84*(3), 475–482. https://doi.org/10.1093/ajcn/84.3.475

Wong, T. S., & Booth, F. W. (1988). Skeletal muscle enlargement with weight-lifting exercise by rats. *Journal of Applied Physiology*, *65*(2), 950–954. https://doi.org/10.1152/jappl.1988.65.2.950

Yan, Z., Okutsu, M., Akhtar, Y. N., & Lira, V. A. (2011). Regulation of exercise-induced fiber type transformation, mitochondrial biogenesis, and angiogenesis in skeletal muscle. *Journal of Applied Physiology*, *110*(1), 264–274. https://doi.org/10.1152/japplphysiol.00993.2010

Yarasheski, K. E., Lemon, P. W., & Gilloteaux, J. (1990). Effect of heavy-resistance exercise training on muscle fiber composition in young rats. *Journal of Applied Physiology*, *69*(2), 434–437. https://doi.org/10.1152/jappl.1990.69.2.434

Young, W. B. (2006). Transfer of strength and power training to sports performance. *International Journal of Sports Physiology and Performance*, *1*(2), 74–83. https://doi.org/10.1123/ijspp.1.2.74

Zhu, W. G., Hibbert, J. E., Lin, K. H., Steinert, N. D., Lemens, J. L., Jorgenson, K. W., Newman, S. M., Lamming, D. W., & Hornberger, T. A. (2021). Weight Pulling: A Novel Mouse Model of Human Progressive Resistance Exercise. *Cells*, *10*(9), 2459. https://doi.org/10.3390/cells10092459

Zwetsloot, K. A., Shanely, R. A., Godwin, J. S., & Hodgman, C. F. (2021). Phytoecdysteroids accelerate recovery of skeletal muscle function following in vivo

eccentric contraction-induced injury in adult and old mice. *Frontiers in Rehabilitation Sciences*, *2*. https://www.frontiersin.org/article/10.3389/fresc.2021.757789

Zwetsloot, K. A., Westerkamp, L. M., Holmes, B. F., & Gavin, T. P. (2008). AMPK regulates basal skeletal muscle capillarization and VEGF expression, but is not necessary for the angiogenic response to exercise: AMPK and the skeletal muscle angiogenic response to exercise. *The Journal of Physiology*, *586*(24), 6021–6035. https://doi.org/10.1113/jphysiol.2008.159871

Vita

Pieter Jan Koopmans was born in Watertown, Wisconsin, to Constance and Pieter Roelof Koopmans. He graduated from Waunakee High School in Wisconsin in June 2015. The following autumn, he entered University of Wisconsin- La Crosse to study Exercise and Sport Science, and in May 2019 he was awarded the Bachelor of Science degree. In the spring of 2019, he accepted a research assistantship in Exercise Science at Appalachian State University and began study toward a Master of Science degree, which was completed in May of 2022. In the Fall of 2022, he will go on to pursue a Ph.D. in Cell and Molecular Biology at the University of Arkansas, where he has been awarded a graduate research assistantship and a Doctoral Academy Fellowship to study molecular mechanisms of muscle mass regulation.